THE POSSIBLE INVOLVEMENT OF SIK2 IN DIABETIC RETINOPATHY

by

Burcu Ersoy

B.S., Molecular Biology and Genetics, Bilkent University, 2012

Submitted to the Institute for Graduate Studies in
Science and Engineering in partial fulfillment of
the requirements for the degree of
Master of Science

Graduate Program in Molecular Biology and Genetics
Boğaziçi University

2015

To my family…

ACKNOWLEDGEMENTS

First and foremost, I would like to express my deepest gratitude to my thesis supervisor Prof. Kuyaş Buğra for her valuable criticism, guidance and patience throughout the project. Being a member of her research group is an exceptional experience for me.

I am very grateful to my committee members, Assist. Prof. Necla Birgül-İyison and Prof. Uygar Tazebay, who took their most valuable time to evaluate my thesis. It is an honor to receive feedback from them about my study.

I would like to thank our former laboratory member Gamze Küser Abalı. My whole study grounds on her valuable findings. I would like to express my special thanks to Neslihan Zöhrap and Aslı Uğurlu for their great support and friendship. They were always available for my questions and they shared generously their valuable time and knowledge with me. Without their help, my research would not have been possible. I would like to thank my lab member and great friend, Emirhan Taşöz. He always motivated me and guided supportively throughout my project.

I would like to express my sincere thanks to my friends and lab mates Burçak Özeş, Mahmutcan Hız, İsmail Tuğberk Kaya, Harun Niron, Büşra Şimşek, Elif Begüm Gökerküçük, Cansu Küey, Ayşe Candayan, Oğuz Arı, Ahmet Burak Kaya, Mustafa Yalçınkaya and Serhat Iştın for their endless support inside and outside the laboratory. I would like to thank again Serhat, Begüm and Cansu for their precious friendship and moral support.

The last but not the least, I have special thanks to my family members for their endless love and encouragement throughout my life.

I would like to thank to The Scientific and Technological Research Council of Turkey 2210-National Scholarship Program and TÜBİTAK 114Z240 fund for granting me. I also appreciate Scientific Research Project (BAP) for financially supporting me and this project (14B01M8).

ABSTRACT

THE POSSIBLE INVOLVEMENT OF SIK2 IN DIABETIC RETINOPATHY

Diabetic Retinopathy (DR) is one of the most common complications of diabetes and in advanced stages it is characterized by vascular abnormalities and neuronal degeneration. It is widely accepted that the functional changes in retinal Müller glia, collectively named as gliosis, constitutes an important factor leading to the dysfunction and degeneration of neurons in the development of DR. Our earlier research indicated that chronic hyperglycemia results in decrease in insulin-dependent survival of cultured Müller cells with concomitant increase in SIK2 activity and expression. Further studies suggest that SIK2 may act as a negative regulator of insulin-induced survival pathway and contributes to hyperglycemia-induced death of Müller glia through downregulation of IRS1 activation *in vitro*. These findings raise the possibility that hyperglycemia induced upregulation of SIK2 expression and/or activity may contribute to development of DR. In this study, to provide evidence towards potential involvement of SIK2 in DR, we investigated modulation of its expression and activity under hyperglycemic conditions using Streptozotocin-induced DR model rats. Analysis of 2-week, 4-week, 8-week diabetic and the age-matched control retinae showed that gliosis of Müller cells gradually increased and spanned the entire thickness of the retina by time, beginning from the 2^{nd} week of diabetes. On the other hand, cell death in retina was first observed in ganglion cells within 4 weeks of diabetes onset then became apparent in Müller cells and neurons of inner nuclear layer in the 8^{th} week of diabetes. Although SIK2 level and expression pattern in the retina showed no change in response to diabetes, its activity seemed to be transiently increased in 2-week and 4-week diabetic retina. No change in SIK2 activity was observed in 8-week diabetic retina compared to control retina. Moreover, co-Immunoprecipitation results demonstrated that SIK2 and IRS1 interaction was upregulated beginning from the 4^{th} week of diabetes supporting the possibility that IRS1 can be negatively regulated by SIK2 leading to the impairment of insulin-induced cell survival in diabetic retina.

ÖZET

SIK2'NİN DİYABETİK RETİNOPATİ'DEKİ OLASI ROLÜ

Diyabetik Retinopati (DR), diyabetin en çok bilinen komplikasyonlarından biridir ve ileri safhalarında nöron dejenerasyonu ve bir takım damarsal anormalliklerle karakterize edilmektedir. Retinadaki Müller gliyanın fonksiyonel değişikliklerinin tümünü kapsayan gliyozisin, DR gelişiminde nöronların fonksiyon bozukluğu ve dejenerasyonuna sebep olan öncü bir faktör olması yaygın olarak kabul gören bir kanıdır. Önceki çalışmalarımız göstermiştir ki kronik hiperglisemi SIK2'nin ifade ve aktivite artışıyla beraber kültür ortamındaki Müller hücrelerinin insüline bağlı sağkalımının azalmasına yol açmaktadır. Daha sonraki *in vitro* çalışmalarımız, SIK2'nin IRS1 aktivitesini baskılaması yoluyla insülinle indüklenen sağkalım yolağının negatif regülatörü görevi gördüğünü ve hiperglisemi ile indüklenen Müller gliya ölümüne katkı sağladığını ileri sürmüştür. Bu bulgular hiperglisemi ile indüklenen SIK2'nin ifade ve/veya aktivite artışının DR'nin ilerlemesine katkı sağlama olasılığını yükseltmektedir. Bu çalışmada, SIK2'nin DR'deki olası rolüne delil ileri sürmek için Streptozotocin'le sıçanlar üzerinde geliştirilen DR modelinde SIK2'nin hiperglisemi altında ifade ve aktivite modülasyonunu inceledik. Öncelikle; 2,4,8 haftalık diyabetik ve kontrol retinalarının analizi göstermiştir ki Müller hücrelerinin gliyozisi diyabetin 2. haftasından itibaren başlamak suretiyle aşamalı olarak artarak bütün retinayı kaplamaktadır. Hücre ölümleri de diyabetin 4. haftasında ilk olarak ganglion hücrelerinde görülmüş, diyabetin 8. haftasında da Müller hücreler ve retinanın iç çekirdek tabakasındaki nöronlarda gözlemlenmiştir. Aynı süre içerisinde diyabetik koşullara karşılık SIK2'nin miktar ve retinadaki ifade ediliş şeklinde bir değişiklik olmamasına rağmen, 2 ve 4 haftalık diyabetik retinadaki aktivitesinde geçici bir artış varmış gibi görülmektedir. Ancak 8 haftalık diyabet ve kontrol retinasını kıyasladığımızda SIK2 aktivitesinde bir değişiklik gözlemlenmemektedir. Ek olarak, ko-immünçökelme sonuçları da göstermiştir ki SIK2 ve IRS1 etkileşimi diyabetin 4. haftası itibariyle artmakla beraber, bu sonuç diyabetik retinada SIK2'nin IRS1'i negatif modüle ederek insülin uyarımlı sağkalım yolağının bozulmasına sebep olma olasılığını da desteklemiştir.

TABLE OF CONTENTS

LIST OF FIGURES

LIST OF TABLES

LIST OF ACRONYMS/ABBREVIATIONS

ACTH	Adenocorticotropic Hormone
ADP	Adenosine Diphosphate
AMPK	AMP-activated Kinase
APS	Amonium Persulfate
ATP	Adenosine Triphosphate
BAD	Bcl-2-associated Death
BAT	Brown Adipose Tissue
BCA	Bicinchoninic Acid
bp	Base Pair
BrdU	Bromodeoxyuridine
BSA	Bovine Serum Albumine
$CaCl_2$	Calcium Chloride
cAMP	Cyclic Adenosine 5'-Monophosphate
CBP	CREB Binding Protein
cDNA	Complementary DNA
chREBP	Carbohydrate Responsive Element-Binding Protein
c-Nap1	Chromosome Condensation-related SMC-associated Protein 1
CNS	Central Nervous System
Co-IP	Co-Immunoprecipitation
CO_2	Carbondioxide

COS	CV-1 in Origin carrying the SV40 genetic material
CRALBP	Cellular Retinaldehyde Binding Protein
CRE	Carbapenem-resistant Enterobacteriaceae
CREB	CRE Binding Protein
DABCO	1,4-Diazabicyclo[2.2.2]octane
DAG	Diacylglycerol
DAPI	Diaminophenylindolamine
DEPC	Diethylpyrocarbonate
dl	Deciliter
DMEM	Dulbecco's Modified Eagle Medium
DNA	Deoxyribonucleic Acid
dNTP	Deoxyribonucleotide Triphosphate
DR	Diabetic Retinopathy
DTT	Dithiothreitol
EDTA	Ethylenediaminetetraacetic Acid
EGTA	Ethylene Glycol Tetraacetic Acid
ERK	Extracellular Regulated Kinase
FBS	Fetal Bovine Serum
FGF	Fibroblast Growth Factor
FGFR	Fibroblast Growth Factor Receptor
FKHR	Forkhead in Rhabdomyosarcoma
FRS2	Fibroblast Growth Factor Receptor Substrate

g	Gram
GAB1	Grb2-Associated Binder 1
GABA	*Gamma*-Aminobutyric Acid
GCL	Ganglion Cell Layer
GFAP	Glial Fibrillary Acidic Protein
GFP	Green Fluorescent Protein
GLUT2	Glucose Transporter 2
GS	Glutamine Synthase
GSK	Glycogen Synthase Kinase
GST	Glutathione S Transferase
GTP	Guanosine-Triphosphate
HCL	Hydrochloric Acid
H_2O	Water
HRP	Horse Radish Peroxidase
IHC	Immunohistochemistry
IgG	Immunoglobulin G
IKKβ	Inhibitor of Nuclear Factor Kappa-B Kinase Subunit βeta
INL	Inner Nuclear Layer
IP	Immunoprecipitation
IPL	Inner Plexiform Layer
IR	Insulin Receptor
IRS	Insulin Receptor Substrate

IVK	*In Vitro* Kinase
JNK	C-Jun N-Terminal Kinase
kb	Kilobase
KCL	Potassium Chloride
KD	Kinase Domain
kDa	Kilodalton
kg	Kilogram
KI	Kinase Inactive
LKB1	Liver Kinase B 1
Lys	Lysine
M	Molar
MAPK	Mitogen-Activated Protein Kinase
Met	Methionine
mg	Miligram
$MgCl_2$	Magnesium Chloride
MIO-M1	Moorfields/Institute of Opthalmology-Müller 1
ml	Mililiter
mm	Milimeter
mM	Milimolar
Mn	Manganase
$MnCl_2$	Manganese Chloride
mRNA	Messenger Ribonucleic Acid

mTOR	Mammalian Target of Rapamycin
NaCl	Sodium Chloride
NADPH	Nicotinamide Adenine Dinucleotide Phosphate Hydrogen
nm	Nanometer
NMDA	N-Methyl-D-Aspartate
ng	Nanogram
NP-40	Nonidet P-40
OCT	Optimal Cutting Temperature compound
OD	Optical Density
ONL	Outer Nuclear Layer
OPL	Outer Plexiform Layer
PAGE	PolyAcylamide Gel Electrophoresis
pAkt	Phospho-Akt
PBS	Phosphate Buffered Saline
PDK1	Phosphoinositide-dependent Protein Kinase 1
pERK	Phospho-Extracellular Regulated Kinase
PFA	Paraformaldehyde
pg	Picogram
PH	Plekstrin Homology
PI3K	Phosphoinositide 3-Kinase
PIP2	Phosphatidylinositol 4,5-Bisphosphate
PIP3	Phosphatidylinositol (3,4,5)-Triphosphate

PKA	Protein Kinase A
PKB	Protein Kinase B
PKC	Protein Kinase C
PLCγ	Phospholipase C-gamma
pM	Picomolar
pm	Picomol
pSer	Phophoserine
PTB	Phosphotyrosine Binding
pThr	Phosphothreonine
PTPase	Protein Tyrosine Phosphatase
pTyr	Phosphotyrosine
PVDF	Polyvinylidene Fluoride
RGC	Retinal Ganglion Cells
RNA	Ribonucleic Acid
RPE	Retinal Pigment Epithelium
rpm	Revolutions per Minute
RTK	Receptor Tyrosine Kinase
SDS	Sodium Dedocyl Sulfate
SDS-PAGE	SDS- Polyacrylamide Gel Electrophoresis
Ser	Serine
SH	Src Homology
SHP2	Sh2-Domain Containing Phosphatase 2

SIK	Salt Inducible Kinase
siRNA	Small Interfering RNA
SOS	Son of Sevenless
STZ	Streptozotocin
TBS	Tris Buffered Saline
TBST	Tris Buffered Saline Tween
TEMED	Tetramethylethylenediamine
Thr	Threonine
TNFα	Tumor Necrosis Factor α
TORC2	Transducer of Regulated CREB Activity
Tyr	Tyrosine
UBA	Ubiquitin-Associated
μm	Micrometer
UTR	Untranslated Region
UV	Ultraviolet
V	Volt
WB	Western Blot
VEGF	Vascular Endothelial Growth Factor

1. INTRODUCTION

1.1. Retina

Retina is light-sensitive neural tissue that lines back of the eye. Vertebrate retina contains three nuclear layers separated by two plexiform layers (Figure 1.1). Photoreceptors, which involve rods and cones, are located in the outer nuclear layer (ONL), the outermost part of the retina, while ganglion cells occupy the innermost nuclear layer (the ganglion cell layer). The nuclei of the remaining neuronal cell types (the horizontal, bipolar and amacrine cells) and Müller glial cells constitute the inner nuclear layer (INL) of the retina, which is located between ONL and ganglion cell layer (GCL) (Smith *et al*., 2002; Centanin and Wittbrodt, 2014). Synaptic transmissions linking the photoreceptors with bipolar cells are modulated by horizontal cells, which face the outer plexiform layer (OPL) (Kolb, 2003; Centanin and Wittbrodt, 2014). Photoreceptors are also in contact with amacrine and ganglion cells (Hoon *et al*., 2014). On the other hand, amacrine cells, which face the inner plexiform layer, contact also with ganglion cells in inner plexiform layer (IPL) (Kolb, 2003).

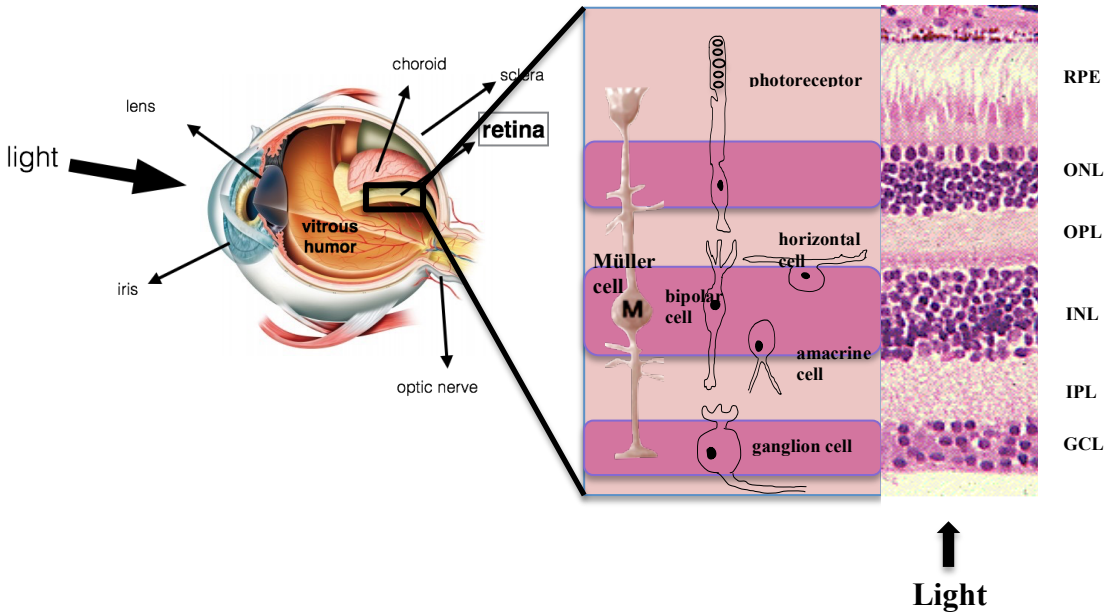

Figure 1.1. The vertebrate eye and magnified layered structure of the retina (modified from Kolb, 1995).

Neurons and glial cells of the retina work in an orderly manner to convert visual information into nerve impulses (Kolb, 2003). In the retina, the light is first detected by photoreceptors and this visual information is converted to membrane potential by the change of neurotransmitter release (Rieke *et al*., 1998; Hoon *et al*., 2014). Ganglion cells transfer the visual information received from bipolar and amacrine cells to higher visual centers in the brain by their axonal projections (Schiller, 2010).

Müller cells are the main glial cells of the vertebrate retina. Although the cell bodies of the Müller cells locate in the INL, their processes reach out the whole thickness of the retina (Figure 1.1) (Bringmann *et al*., 2006). Müller cells are in contact with retinal neurons, blood vessels, the vitreous body and the subretinal space (Bringmann *et al*., 2006). Outer limiting membrane of the retina is formed by the specialized junctions between Müller cells and photoreceptor cell inner segments (Garcia and Vecino, 2003). Inner limiting membrane is formed by laterally contacting Müller cell end feet and associated basement membrane constituents. Müller cells also support the structural organization of blood-retina barrier (Garcia and Vecino., 2003). Considering the importance of the connections of Müller cells, it has been reported that they play a significant role in support, homeostasis and the activity of retinal neurons (Bringmann *et al*., 2006; Garcia and Vecino., 2003). They express many of the ligand receptors, ion channels, transporter molecules and specific enzymes for proper functioning (Newman and Reichenbach, 1996; Sarthy and Ripps, 2001). Müller cells are involved in glucose, ion and water metabolism, removal of metabolic waste products, regulation of blood flow, neuronal signaling process (uptake and recycling of neurotransmitters), activity and survival by providing trophic factors (Bringmann *et al*., 2006).

1.2. Diabetic Retinopathy

Diabetes is a metabolic disease that causes high circulating glucose affecting several organs, including the eye and retina (Ola *et al*., 2012). Diabetic Retinopathy (DR) is an eye disease characterized by a cascade of events such as gliosis, cell dysfunction/death, microaneurysms, leakage of blood into the retinal tissue and vitreous in the eye eventually leading to blindness (Miyamoto *et al*., 1999; Barber *et al*., 2005). Diabetes affects not only retinal vasculature, but also function, integrity and morbidity of retinal neuronal and glial cells (Barber *et al*., 1998; Martin *et al*., 2004). It has been reported that up to 80 percent of

10-year diabetic patients are affected by DR (Kertes *et al*., 2007) and after 15 years of having diabetes, 98 percent of type 1 diabetic patients and 78 percent of type 2 diabetic patients have some degree of retinal damage and in fewer than 5 percent of diabetic people, severe vision loss has been observed (Engelgau *et al*., 2004; Williams *et al*., 2004). As an estimated number, 92,6 million adults around the world are affected by DR (Yau *et al*., 2012).

In DR, high circulating glucose leads to overproduction of superoxides and increased oxidative stress by depletion of NADPH in polyol pathway (Jiang *et al*., 2013; Ola *et al*., 2012). Attenuated expression of antioxidant enzymes such as Mn-containing superoxide dismutase, glutathione peroxidase and catalase in hyperglycemia has been reported to be involved in retinal cell dysfunction and degeneration (El-Bab *et al*., 2013). These metabolic changes arising from elevated glucose give rise to the dysfunction and apoptosis of Müller cells and retinal neurons by inactivation of Akt survival pathway (Xi *et al*., 2005). In addition to metabolic changes and the increase in reactive oxygen species, the failure of insulin-induced Akt survival pathway has great contribution in retina degeneration under hyperglycemia (Reiter *et al*., 2003). Insulin receptors (IRs) and their downstream effectors such as Insulin Receptor Substrate-1/2 (IRS-1/2) and phosphatidylinositol-3-kinases (PI3Ks) are widely distributed throughout the central nervous system (CNS) including retina (Rajala *et al*., 2009). It has been proposed that inactivation of any of these elements leads to Akt inactivation and consequently dephosphorylation of the Bcl-2-associated death promoter (BAD), increased cytochrome c release, and activation of caspase-3 and caspase-9, which are essential for programmed cell death (Xi *et al*., 2005).

1.2.1 Müller Cell Gliosis in DR

Response of Müller cells to pathological alterations in the retina influences whole tissue, since these cells are the key players supporting neuron survival and function. The reactive changes of Müller cells upon retinal injury and chronic neuronal stress are called Müller cell gliosis (Dyer *et al*., 2000). Like other glial cells of the CNS, Müller cell gliosis can be characterized by both non-specific responses independent of given stimulus and specific responses that depend on the existing pathogenic factor or mechanism (Bringmann

et al., 2006). Many retinal diseases including DR, hepatic retinopathy, retinitis pigmentosa, macular degeneration and proliferative vitreoretinopathy are associated with Müller cell gliosis (Bringmann and Reichenbach, 2001). Although early after injury gliosis seems to be neuroprotective by providing the release of neurotropic factors and antioxidants, at later stages it leads to impairment of supportive functions of Müller cells causing the further progression of the disease (Bringmann *et al*., 2006). The upregulation of the intermediate filament protein, glial fibrillary acidic protein (GFAP), which participates in modifying cellular structure and glial networks, is considered to be early cellular marker for retinal diseases (Bignami and Dahl, 1979; Eisenfeld *et al*., 1984; Bringmann and Reichenbach, 2001).

Neuron dysfunction and death in the diabetic retina can be attributed to Müller cell gliosis. The increase in GFAP expression, which is mostly associated with changes in cell morphology, is observed early on the course of the diabetes and precedes the onset of vascular changes (Bringmann *et al*., 2006). In addition to GFAP upregulation, in hyperglycemic animals several functions of Müller cells are lost leading to disruption of potassium, glycine and glutamate homoeostasis, accumulation of *gamma*-Aminobutyric acid (GABA), upregulation of pro-inflammatory cytokines, increased expression of angiogenic growth factors and breakdown of blood-retinal barrier (Lieth *et al*., 1998; Barber *et al*., 2000; Rungger-Brandle *et al*., 2000). Within the healthy Müller glia, Glutamine Synthetase (GS), a Müller cell specific enzyme, converts neurotransmitter glutamate to glutamine so that it can re-enter the extracellular space as a non-neuroactive substance and can be rapidly taken into neurons for ongoing neuronal signaling (Pow and Robinson, 1994). However, upon gliosis, glutamate/glutamine cycle is broken resulting in accumulation of glutamate and neurodegeneration in the retina (Lieth *et al*., 2000). Therefore, Müller glia dysfunction/death due to diabetes contributes to neuronal and vascular complications, eventually leading to development of DR.

1.2.2. Cell Death in STZ-Induced DR Models

Streptozotocin (STZ, 2-deoxy-2-(3-(methyl-3- nitrosoureido)-D-glucopyranose) is a chemical reagent widely used to induce experimental diabetes in animals. Researchers use STZ extensively in animal models to study both the pathology and complications of the

diseases including DR (Deeds *et al*., 2011). STZ is very toxic to pancreatic β cells because of its alkylating agent properties and the main reason for its specificity is the affinity of STZ to glucose transporter GLUT2 that is mainly found in pancreatic β cell membranes (Xu *et al*., 2008). In addition to its lethal effect to insulin producing pancreatic β cells, STZ also prevents glucose oxidation (Bedoya *et al*., 1996) and decreases insulin biosynthesis and secretion (Bolaffi *et al*., 1987; Nukatsuka *et al*., 1990).

Since retina consists of various types of cells, the characteristic of the cell type and its position in the visual processing pathway could be critical factors determining differential sensitivity of the cells to the same stimulus. Thereby, each cell type in the retina can respond in different way and time to diabetes. It is suggested that retinal cell death occurs mostly by apoptosis considering that dying cells show typical characteristics of apoptosis such as fragmentation of cell nuclei (Barber *et al*., 1998) In STZ-induced hyperglycemia, it has been reported that the earliest time when apoptotic cells are observed due to hyperglycemia is 3-4 weeks after the onset of diabetes and these cells mostly include ganglion cells (Barber *et al*., 1998; Oshitari *et al*., 2005). Ganglion cell loss is estimated to be about 15% after 1 month and 20% after 4 months of STZ induction compared with the age-matched control rats (Zeng *et al*., 2000). Although there is a study suggesting that apoptosis appeared in a few photoreceptor cells in 4^{th} week of diabetes, apoptotic nuclei were rarely observed among the photoreceptor cells even in the 8-week diabetic retina but remarkable in 12-week and 24-week diabetic retinae (Park *et al*., 2003). In the same study it was indicated that in the 12-week diabetic retina some amacrine cells showed necrotic features. Within 15 weeks of diabetes, the increase in pericyte cell loss and capillary occlusion were observed as well (Hammes *et al*., 1995). The number of apoptotic neurons in the INL was increased by more than 50% in 4 months and older diabetic rats (Zeng *et al*., 2000). However, there is still lack of information about the faith of Müller cells and other neurons of retina namely bipolar, amacrine and horizontal cells in the early course of diabetes. Müller glia apoptosis and the mechanism leading to metabolic changes under the early hyperglycemic conditions have not been fully understood yet.

1.3. Insulin Signal Transduction Pathways

Insulin is a metabolic hormone secreted by pancreatic β cells to maintain the homeostasis of circulating blood glucose in mammals (Kanzaki *et al*., 2001). In addition to glucose metabolism, it functions in the control of cell survival and differentiation where the PI3K-Akt and Ras/ERK pathways are the main signaling routes, respectively (Kanzaki *et al*., 2001; Küser-Abalı *et al*., 2013). IR, which is a receptor-tyrosine kinase, is composed of two extracellular α-subunits and two transmembrane β-subunits linked by disulfide bonds (Figure 1.2) (Czech, 1985; Kanzaki *et al*., 2001).

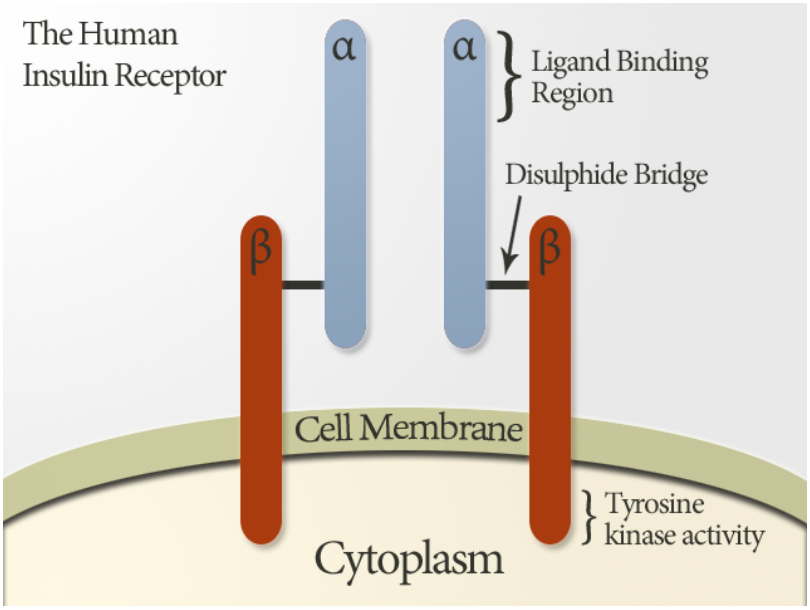

Figure 1.2. Structure of insulin receptor. (Adapted from Ullrich *et al*., 1985).

Insulin binding to its receptor induces receptor dimerization and results in trans-autophosphorylation reactions (Pessin and Alan, 2000). It has been reported that phosphorylation of different tyrosine residues on IR can be associated with distinct functions. For instance, phosphorylation of COOH-terminal tyrosines evokes mitogenic actions whereas Tyr-phosphorylation on juxtamembrane domain can lead to downstream effector binding (Pessin and Alan, 2000). In general, activation of these phosphorylation events results in two discrete biological effects, which are metabolic and growth & differentiation-promoting effects (Madonna *et al*., 2012). The activation of IRSs dock downstream effectors, which later on activate different signaling pathways such as ERK pathway, which is involved in growth and differentiation or PI3K, which is mainly involved in metabolic actions and survival (Gual *et al*., 2005). Metabolic effects, in which

PI3K/Akt pathway is responsible, include glucose uptake and transport, glycogen and protein synthesis and inhibition of lipolysis (Madonna *et al*., 2012). Insulin has also anti-inflammatory effect in the maintenance of blood vessel homeostasis by providing the release of nitric oxide (Madonna *et al*., 2012).

Retinal insulin signaling is crucial for retinal physiology, contributes to retinal development and provides trophic support for cell survival in the adulthood (Hernandez-Sanchez *et al*., 1995). It has been shown that retinal cells express high levels of IRs and IRSs comparable to the liver and brain (Reiter *et al*., 2003). All three isoforms of Akt proteins are expressed in the retina but only Akt-1 has been shown to be activated by insulin signaling (Reiter *et al*., 2003). There is an evidence indicating that Müller glial cells of the retina contained insulin specific mRNA, so it drew attention to extrapancreatic insulin synthesis (Das *et al*., 1987).

1.3.1. Insulin-Induced PI3K/Akt/Survival Pathway

Upon insulin binding, insulin receptor undergoes autophosphorylation on specific tyrosine residues and stimulates kinase activity (Sun *et al*., 1993). The essential element of insulin response, IRS1, which is around 185-kDa protein, is one of the target proteins of IR (Sun *et al*., 1993). Multiple tyrosine-containing motifs on IRS1 are detected and phosphorylated by IR (Sun *et al*., 1993). Phosphorylation of these Tyr residues results in a specific and strong association between IRS1 and SH2 domains in p85, regulatory subunit of PI3K, that in turn forms a docking site for the catalytic subunit, p110 at the membrane (Figure 1.3) (Madonna et al., 2012; Sun *et al*., 1993). P110 participates in the conversion of phosphatidylinositol 4,5-bisphosphate (PIP2), a trans-membrane lipid, into a second messenger phosphatidylinositol 3,4,5-trisphosphate (PIP3). (Vivanco *et al*., 2002). Generation of PIP3 activates phosphoinositide-dependent protein kinase 1 (PDK1) and recruits Akt (also known as protein kinase B) to the cell membrane (Vivanco *et al*., 2002). PDK1 and mTOR/Rictor complex mediate the phosphorylation of Akt on its Thr308 and Ser473 residues, respectively (Dummler and Hemmings, 2007). Akt, which is a serine/threonine kinase, has an amino-terminal PH domain, a central catalytic domain and a short carboxyl-terminal regulatory domain (Vivanco *et al*., 2002). Although there are three isomers of Akt, Akt1 is the one that functions in the cell growth and anti-apoptotic

pathway (Chen *et al*., 2001). Activated Akt1 directly phosphorylates some members of cell-death machinery such as BAD, Caspase 9 and FKHR (a member of the Forkhead family of transcription factors), consequently inhibits their proapoptotic function (Vivanco *et al*., 2002).

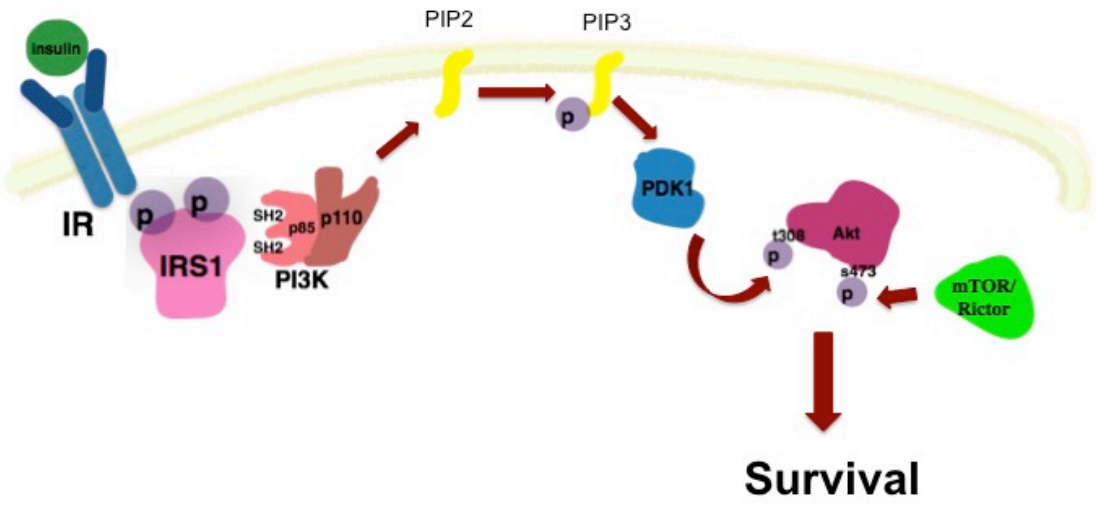

Figure 1.3. Insulin-induced PI3K/Akt survival pathway.

Activity of insulin induced PI3K/Akt/survival pathway can be negatively regulated by phosphatases and serine/threonine kinases (Chang *et al*., 2003; Qiao *et al*., 2002). Several tyrosine phosphatases (PTPases) can dephosphorylate the IR in turn hamper insulin action. A number of Ser/Thr kinases including PKC isoforms, are activated and target IR or its substrates to attenuate insulin signaling (Considine *et al*., 1995). Insulin also induces phosphorylation of IRS1 on serine residues via activation of several kinases in turn activates its own negative feedback mechanism (Gual *et al*., 2005). IRS proteins have more than 70 Ser/Thr residues that are potential targets for phosphorylation thereby causing inhibition of IRS activity and eventually rendering animals resistant to insulin stimulation (Horike *et al*., 2003; Zick, 2005). It has been suggested that Ser/Thr phosphorylation of IRS proteins downregulates its action in insulin signaling through blocking its Tyr phosphorylation thus interfering with the formation of IRS-IR and IRS-downstream effectors (Mothe *at al*., 1996). It has also been suggested that Ser/Thr phosphorylation of IRS1 in hyperglycemic adipocytes triggers degradation of IRS1 proteins (Pederson *et al*., 2001). In addition, decreased IRS1 protein has been observed in some insulin resistant animal models (Kerouz *et al*., 1997) and *in vitro* cell culture models

exposed to chronic stimulation with insulin (Ricort *et al*., 1995) or tumor necrosis factor (TNFα) (Stephens *et al*., 1997).

Apart from Ser/Thr phosphorylation of IRS proteins, negative regulation of the pathway includes Akt degradation. It has been reported that Akt protein is cleaved by active caspases namely caspase-3, -6, and -7 *in vitro*, leading to the loss of the C-terminal domain and reduced kinase activity during TNFα-induced apoptosis (Medina *et al*., 2005).

In this context, identification of several Ser/Thr kinases including SIK2, a member of the Salt Inducible Kinase (SIK) family, which are responsible for the serine phosphorylation of IRS1 protein, is gaining attention as modulators of the negative feedback mechanism in insulin signaling (Horike *et al*., 2003; Küser-Abalı *et al*., 2013).

1.4. Salt Inducible Kinase Family

The SIK family, which belongs to the family of AMP-dependent protein kinases, has three SIK proteins namely SIK1, SIK2 and SIK3 (Bright *et al*., 2009). SIK1 is mainly expressed in adrenal gland and in lower amounts in ovary, brain, testis, and skeletal muscle (Horike *et al*., 2003). It is present in both nucleus and cytoplasm in the cell. SIK1 is known to regulate the steroidogenic gene expression at the early stage of Adrenocorticotropic hormone (ACTH) signaling in adrenocortical cells (Katoh *et al*., 2004). It also participates in liver glucose homeostasis and myocyte survival (Ko *et al*., 2005; Berdeaux *et al*., 2007). SIK2, on the other hand, is largely expressed in both white adipose and brown adipose tissue, and in small amounts in the testis (Horike *et al*., 2003). It was also shown to be widely expressed in vertebrate retina (Figure 1.4) and cultured Müller glia (Küser-Abalı *et al*., 2013). It localizes in nucleus but mostly in cytoplasm. SIK2 is originally has been implicated to play important roles in adipose differentiation (Horike *et al*., 2003). SIK3 was shown to be ubiquitously expressed (Okamoto *et al*., 2004). A recent work indicated that SIK3 regulates cholesterol and bile acid metabolism, and may modulate the size of energy storage in mice (Uebi *et al*., 2012). The genes of *SIK2* and *SIK3* are found on chromosome 11 while the gene of *SIK1* is localized on chromosome 21 (Katoh *et al*., 2004). Molecular characterization of all SIK isoforms revealed that they have similar structural organization with an N-terminal kinase domain containing flexible activation

loops followed by ubiquitin associated (UBA) domain and C-terminal PKA phosphorylation sites (Figure 1.5) (Katoh *et al*., 2004).

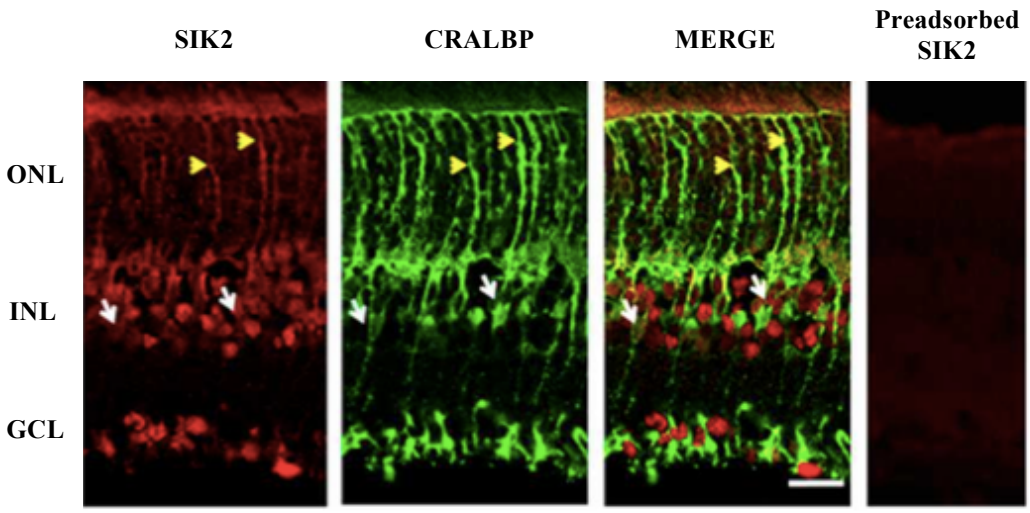

Figure 1.4. Expression of SIK2 in rat retina and Müller cells (Küser-Abalı *et al*., 2013).

1.4.1. SIK2

SIK2 is a serine/threonine kinase with a molecular mass around 120 kDa (Figure 1.5). Lys49 residue of SIK2 located in ATP binding loop is critical for its kinase activity. (Horike *et al*., 2003). SIK2 autophosphorylation activity was shown to be in the A-loop of the kinase domain in transfected COS7 cells but the critical residue has not been identified yet (Hashimoto *et al*., 2008).

SIK2 has been thought to take part in the process of preadipocyte-adipocyte differentiation and its expression and activity were shown to be upregulated in white adipose tissue of db/db diabetic mice (Horike *et al*., 2003). In the liver of genetically insulin resistant rodents, S789 phosphorylation of IRS1 was shown to be increased, suggesting a potential novel serine kinase because this motif was not the target of previously known serine kinases (Qiao *et al*., 2002). It was reported that S789 on IRS1 was the target of SIK2 like AMPK (Horike *et al*., 2003) so identification of IRS1 as a substrate of SIK2 implicates that SIK2 is involved in development of insulin resistance (Horike *et al*., 2003).

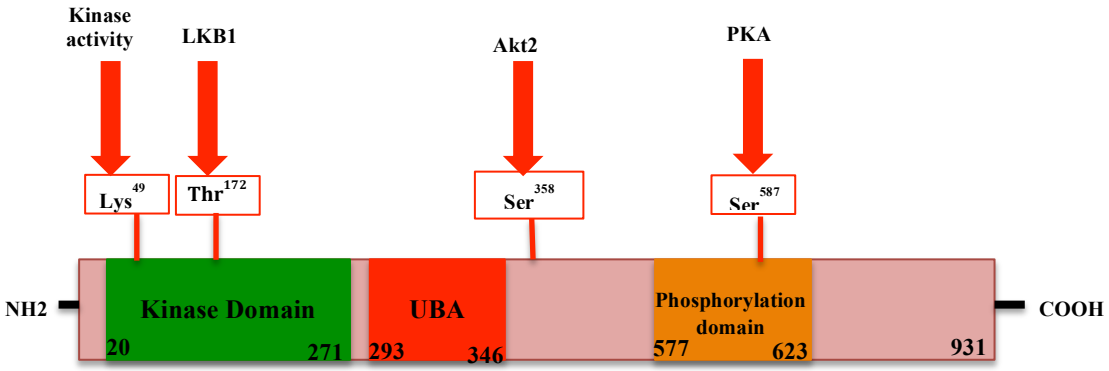

Figure 1.5. Schematic representation of the domains and critical residues of SIK2 protein. Numbers represent the aminoacid numbers.

It was reported that SIK2 increased TORC2:14-3-3 interaction by phosphorylating Ser171 residue on TORC2 thus inhibited CREB function in the regulation of gluconeogenesis (Screaton *et al*., 2004). During fasting of mice, cAMP activity downregulates SIK2 kinase activity via the PKA-mediated phosphorylation of SIK2 at Ser587 (Figure 1.5) (Okamoto *et al*., 2004). During re-feeding, insulin promotes Akt2-mediated phosphorylation of SIK2 at Ser358 and results its activation thereby inhibition of TORC2 activity in gluconeogenic gene expression (Dentin *et al*., 2007). Another known upstream kinase of SIK2 is LKB1, which targets and phosphorylates Thr172 residue in the activation loop of SIK2 and other AMPK-related kinases thus increases the kinase activity of SIK2 *in vitro* (Lizcano *et al*., 2004). It has been suggested that the impairment of LKB1 activity can activate CREB-dependent gene expression by blocking SIK2-mediated phosphorylation of TORC2 (Screaton *et al*., 2004). In addition to liver gluconeogenesis, SIK2 also regulates liver lipogenesis by phosphorylating histone acetyltransferase p300 on Ser89 thus inhibits its activity which in turn reduces ChREBP-mediated lipogenesis in hepatocytes (Bricambert *et al*., 2010).

In recent years, SIK2 has also been reported to be involved in non-metabolic functions. Exposure to UV irradiation causes both downregulation of SIK2 expression and cAMP/PKA-mediated phosphorylation-dependent inactivation of SIK2 activity in turn enhances a CREB-TORC2-dependent melanogenesis of the skin (Horike *et al*., 2010). It was indicated that after ischemic injury SIK2 protein was reduced through its phosphorylation at Thr484 and suppression of SIK2 enhanced neuronal survival via the activation of TORC1-CREB axis (Sasaki *et al*., 2011). It was also suggested that SIK2 was

located at the centrosome and was required in centrosome separation through phosphorylation of c-Nap1 in ovarian cancer cells (Ahmed *et al*., 2010). In the same study, it was demonstrated that depletion of SIK2 in the ovarian cancer cell lines resulted in substantive decrease in cancer cell proliferation. SIK2 was also shown to be involved in autophagy and endoplasmic reticulum (ER)-associated protein degradation (ERAD) through phosphorylation of p97/VCP (Yang *et al*., 2013).

The first indication of SIK2 expression in the retina came from a yeast two-hybrid screen of a retinal cDNA library using the cytoplasmic domain of FGFR2 as bait in our laboratory (Özcan, 2003). The full length SIK2 cloned from rat retinal tissue showed 94 percent of overall identity to mouse and 89.3 percent to human SIK2 (Özcan, 2003; Uysal, 2005). In retina, alternative splicing of the *SIK2* generates 3 isoforms encoding 2 proteins that differ at their carboxyl-terminal (Uysal, 2005).

In further studies, our group showed that SIK2 activity was transiently upregulated upon FGF2 stimulation and SIK2 overexpression resulted in decreased FGF2-dependent ERK and Akt activation via serine phosphorylation Gab1 in Müller cells (Kuser, 2013). On the other hand, SIK2 silencing enhanced the intensity and duration of active ERK and Akt levels leading to increased FGF2-dependent Müller cell proliferation suggesting that SIK2 is involved in the negative feedback mechanisms in FGF/Ras/ERK and FGF/PI3K/Akt pathways and in the negative regulation of Müller cell proliferation through Gab1 serine phosphorylation (Küser, 2013). In the same cells, it was shown that SIK2 activity on IRS1 increased in response to insulin treatment but Akt activation increased thereafter suggesting that SIK2 activation preceded that of Akt in insulin signaling. In the cells grown under chronic hyperglycemia, SIK2 activity was doubled while basal level of active Akt decreased (Küser-Abalı *et al*., 2013). SIK2 overexpression in normal glucose concentrations accelerated Akt inactivation and cell death. As observed in Müller cells grown under hyperglycemic conditions *in vitro,* increase in SIK2 activity was observed in 2-week diabetic rat retina (Küser-Abalı *et al*., 2013). In conclusion, it can be suggested that SIK2 is also involved in the negative regulation of insulin-induced PI3K/Akt pathway and Müller cell survival (Figure 1.6)

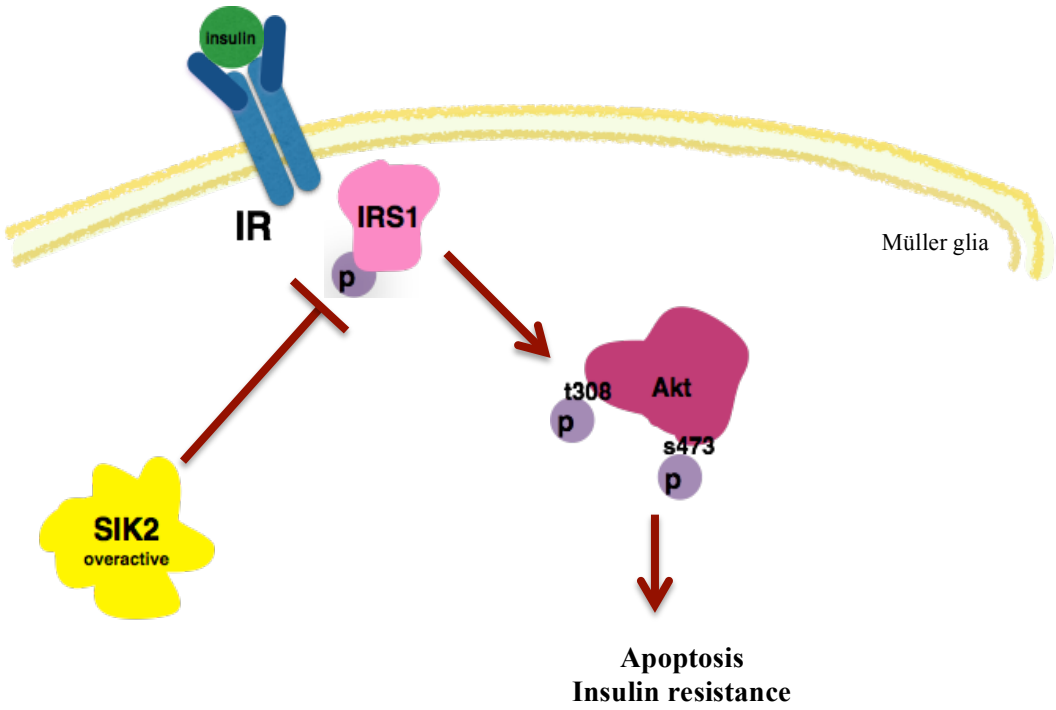

Figure 1.6. Proposed model of SIK2 in insulin resistance in retina (Küser, 2011).

2. AIM OF THE STUDY

In vitro studies performed in our laboratory have suggested that SIK2 acts as a negative modulator of the insulin-dependent survival pathway and contributes to hyperglycemia-induced cell death of Müller glia through serine phosphorylation of IRS1. SIK2 participation may contribute to impairment of insulin signaling via modulations in expression and/or activity level in the retina. Therefore, we aimed to identify the potential involvement of SIK2 in STZ-induced DR.

Towards the objective of this study we performed several experiments listed below: Diabetic rat model was generated with a single dose of STZ injection.

- The alterations in Müller cells of the retina in response to diabetes were analyzed by immunohistochemistry.
- The early time profile of the cell death in diabetic retina was monitored by immunohistochemistry and the apoptotic cells were characterized by double labeling with apoptosis and specific cell markers.
- The modulation in SIK2 protein level in diabetic retina was analyzed by Western Blot analysis.
- The change in the expression pattern of SIK2 between diabetic and control retina was investigated by immunohistochemistry.
- The change in SIK2 activity in diabetic retina was followed by *in vitro* kinase assays.
- SIK2-IRS1 interaction and serine phosphorylation of IRS1 were analyzed via Co-IP and Western Blot analysis, respectively.

3. MATERIALS

3.1. Animals

Male Wistar albino rats with the weights of 300±50 g were used in this study for the generation of *in vivo* DR model. They were obtained from Boğaziçi University, Center for Life Sciences and Technologies. The rats were maintained under pathogen free conditions, 12:12 day:night cycle and appropriate humidity at room temperature. Food and water were provided *ad lib*. All procedures and handling of animals were in accordance with Boğaziçi University Ethics Committee guidelines and approval.

3.2. Chemicals, Plastics and Disposable Glassware

All chemicals used in this study were purchased from Sigma Aldrich Ltd. (USA) or Merck (Germany) unless otherwise stated in the text. All solutions, plastics and disposable glassware were sterilized by autoclaving at 121^0C for 20 minutes when required.

3.3. Kits

Kits used in this study were listed in Table 3.1.

Table 3.1. List of kits used in this study.

Kit	Supplier
Bicinchoninic acid (BCA) assay kit	Thermo, USA
Universal Kinase Activity Kit	R&D Systems, USA

3.4. Antibodies

The following antibodies listed in Tables 3.2 and 3.3 were used throughout this study.

Table 3.2. List of primary antibodies used in this study.

Antigen	Host	Application	Producer
SIK2	Rabbit	IHC, WB, IP, Co-IP	Novus Biologicals
Cleaved Caspase 3	Rabbit	IHC	Cell Signaling
CRALBP	Mouse	IHC	Abcam
HuC/HuD	Mouse	IHC	Life Technologies
GFAP	Mouse	IHC	Santa Cruz Biotechnology
Glutamine Synthetase	Rabbit	IHC	Abcam
IRS1	Rabbit	WB, Co-IP	Cell Signaling
p-IRS1 s789	Rabbit	WB	Cell Signaling
b-Actin	Mouse	WB	Santa Cruz Biotechnology

Table 3.3. List of secondary antibodies used in this study.

Target	Host	Tag	Application	Producer
Rabbit	Donkey	Fluorophore 555	IHC	Invitrogen
Mouse	Donkey	Fluorophore 488	IHC	Invitrogen
Rabbit IgG	Goat	Horse radish Peroxidase	WB	Santa Cruz Biotechnology

3.5. Buffers and Solutions

Buffers and solutions used in this study are listed in Tables 3.4 - 3.7. The contents of these preparations are also given in the tables.

Table 3.4. List of buffers and solutions used in protein extraction and tissue preparation.

Buffer or Solution	**Content**
Citrate Buffer	0.05 M citric acid 0.05 M trisodium citrate (pH: 4.5)
STZ Solution	10% STZ in citrate buffer
Lysis Buffer	20 mM Tris-HCL (pH:7.5) 150 mM NaCL 1 mM EDTA %1 Triton-X
Paraformaldehyde (PFA) Solution	4% PFA in PBS

Table 3.5. List of buffers and solutions used in immunohistochemistry.

Buffer or Solution	**Content**
PBS	10% PBS (10X) in dH_2O
Wash Buffer	0.01% tween-20 in PBS
Permeabilization Buffer	0.1% Triton X-100 in PBS
Blocking Solution	1% glycine 0.1% albumin BSA 0.1% Tween-20 5% donkey serum in PBS

Table 3.5. List of buffers and solutions used in immunohistochemistry (cont.).

Tris-Buffered Saline (TBS)	20 mM Tris-Cl (pH 8.0) 150 mM NaCl
Mounting Medium	2.5% DABCO in glycerol
Sucrose Solutions	10% Sucrose in PBS 20% Sucrose in PBS 30% Sucrose in PBS

Table 3.6. List of buffers and solutions used in Western Blot analysis.

Buffer and Solution	**Content**
Protein Sample Buffer (6X)	300 mM Tris-Cl (pH 6.8) 12 mM EDTA 60% Glycerol 12% SDS 6% β-mercaptoethanol 0.04% Bromophenol blue
TBS with Tween 20 (TBS-T)	0.1% Tween 20 in TBS
SDS-Polyacrylamide Gel (10%)	375 mM Tris-Cl (pH 8.8) 10% Acrylamide:Bisacrylamide (37.5:1) 0.1% SDS 0.1% APS 0.1% TEMED

Table 3.6. List of buffers and solutions used in Western Blot analysis (cont.).

SDS-Polyacrylamide Gel (5%)	125 mM Tris-Cl (pH 6.8) 5% Acrylamide:Bisacrylamide (37.5:1) 0.1% SDS 0.1% APS 0.1% TEMED
Running Buffer	25 mM Tris-Cl 250 mM Glycine 0.2% SDS
Transfer Buffer	25 mM Tris-Cl 200 mM Glycine 15% Methanol

Table 3.7. List of buffers and solutions used in IP and Co-IP assays.

Lysis Buffer for IP	50 mM Tris-HCl (pH 8.0) 150 mM NaCl 1% NP40
Lysis Buffer for Co-IP	20 mM Tris-HCL (pH:7.5) 150 mM NaCL 1 mM EDTA %1 Triton-X
2X SDS Sample Buffer	%4 SDS %20 glycerol %10 B-mercaptoethanol %0.004 bromophenol blue 0.125 M Tris-HCL (pH: 6.8)

3.6. Laboratory Equipment

The list of laboratory equipment used throughout this project is given in Table 3.8.

Table 3.8. List of laboratory equipment used in this study.

Equipment	Producer
Autoclave	Model MAC-601, Eyela, Japan Model ASB260T, Astell, UK
Balances	Electronic Balance VA 124, Gec Avery,USA DTBH 210, Sartorius, GERMANY
Blood glucose meter	GlucoMax, BTI Inc. Industrial Park, Hsinchu, Taiwan
Carbon dioxide tank	2091, Habaş, TURKEY
CCD camera	CCD Camera, JAI Corporation, JAPAN
Centrifuges	Centrifuge 5415 R, Eppendorf, Germany Mini Centrifuge 17307-05 Cole Parmer, USA
Chemiluminescence Detection System	Stella, Raytest, Germany
Confocal Microscope	SP5, AOBS, Leica, Germany
Cryostat	Leica CM3050 S, USA
Deep Freezers	2021D (-20^{0}C), Arçelik, Turkey -70^{0}C Freezer, Harris, UK -86^{0}C ULT Freezer, ThermoForma, USA -152^{0}C ULT Low Freezeri, Sanyo, USA

Table 3.8. List of laboratory equipment used in this study (cont.).

Electrophoretic Equipments	Mini-PROTEAN 3 Cell, BIO-RAD, USA Easy-cast system, Hybaid, UK
Heat blocks	DRI-Block DB-2A, Techne, UK StableTemp Dry Bath Incubator, Cole Parmer, USA
Hybridization Oven	Shake'n'Stack, Hybaid, UK
Ice Machine	Scotsman Inc., AF20, ITALY
Incubator	Hepa Class II Forma Series, Thermo Electron
Laminar flow cabinet	Class II A Tezsan, TURKEY Class II B Tezsan, TURKEY
Magnetic Stirrer	M221 Elekro-mag, TURKEY Clifton Hotplate Magnetic Stirrer, HS31, UK
MagNa Lyser	Roche, GERMANY
Micropipettes	Gilson, FRANCE
Microscopes	CM110 Inverted Microscope, Prior, UK Zeiss, Axio Observer Z1 Inverted Mic., USA
pH meter	WTW, GERMANY
Pipettor	Pipetus-akku, Hirscmann Labogerate, GERMANY
Pipettor	Pipetus-akku, Hirscmann Labogerate, GERMANY
Power Supplies	EC135-90, Thermo Electron Corporation Power Pac Universal, BIO-RAD, USA
Protein Visualization	Stella, Raytest, GERMANY

Table 3.8. List of laboratory equipment used in this study (cont.).

Refrigerators	2082C, Arçelik, TURKEY 4030T, Arçelik, TURKEY
Sealer	Vacuplus FS400A, Electric Petra, GERMANY
Shakers	VIB Orbital Shaker, InterMed, DENMARK Lab-Line Universal Oscillating Shaker, USA Adjustable Rocker, Cole Parmer, USA
Software	Metasystems, GERMANY Quantity One, Bio-Rad, ITALY
Spectrophotometer	CE5502, Cecil, UK NanoDrop ND-1000, Thermo, USA
Water Bath	TE-10A, Techne, UK
Water Purification	UTES, TURKEY
Vortex	Vortexmixer VM20,Chiltern Scientific, UK

4. METHODS

4.1. Induction of Diabetes with STZ Injection in Rats

Adult male Wistar albino rats with an average weight of 300±50 g received a single dose of 60 mg/kg STZ freshly solubilized in citrate buffer (0.05 M citric acid and 0.05 M trisodium citrate, pH: 4.5) by intravenous injection in the tail vein. The concentration of STZ in citrate buffer was 100 mg/ml. Control rats were injected with vehicle alone. The fasting blood glucose levels were monitored on the 2nd day after the injection and only the rats with a basal glucose level above 200 mg/dl were considered diabetic. All rats were fed with normal diet. Their fasting blood sugar levels and weights were measured weekly until the day of sacrifice. Just before the time of sacrifice (day 0, 2 weeks, 4 weeks and 8 weeks after onset of diabetes), the diabetic state of the rats was confirmed again by measuring blood glucose levels with the blood glucose meter (GlucoMax). Experimental and control rats were anesthetized by carbondioxide inhalation and sacrificed by cervical dislocation at the day 0, 2 weeks, 4 weeks and 8 weeks post injection.

4.2. Tissue Preparation

For immunohistochemical stainings using frozen sections, eyes were enucleated, the eyecup was taken to PBS solution and fixed in 4% PFA at 4^{o}C overnight. The tissue was rinsed for 3x10 minutes in ice cold PBS and cryoprotected by incubation in sequential sucrose-PBS dilutions (10%, 20% and 30%) at 4^{o}C. Later on, the retina was embedded in OCT and the sample was flash frozen at -150^{o}C for 5 minutes and stored at -20^{o}C until use.

For the protein analysis, the cup-shaped retina was taken out, freshly frozen and stored -80^{o}C until use.

4.3. Immunohistochemistry

Frozen sections of retina with 12 μm thicknesses were taken onto the positively charged slides with cryostat and stored -20^{o}C until immunolabelling. The slides were rehydrated in PBS, permeabilized with %0.1 Triton X-100 in PBS for 5 minutes at room

temperature. Afterwards the samples were incubated in appropriate blocking solutions given in Table 4.1 for 1 hour at room temperature in order to block non-specific binding sites on samples. The samples were incubated in primary antibodies prepared in desired dilutions in the blocking solution as indicated Table 4.1 overnight at 4^{o}C. The antibody solution was removed and the samples were washed with PBS containing 0.01 % tween-20 for 4x10 minutes. Subsequent to extensive washing, the samples were incubated with appropriate fluorescent dye conjugated secondary antibodies for 1 hour at room temperature in the dark. DAPI labeling was performed using 0.05 µg/ml DAPI in TBS for 5 minutes. After washing the sections 3x10 minutes each, the slides were mounted and sealed with nail polish. Prepared slides were stored at 4^{o}C until imaging.

Table 4.1. List of antibodies and their working solutions used in immunohistochemistry.

	Antibody	**Host**	**Blocking**	**Dilution**
Primary antibodies	Anti-SIK2	Rabbit polyclonal	%5 donkey serum in blocking solution	1:250
	Anti-cleaved Caspase 3	Rabbit polyclonal	%10 donkey serum in blocking solution	1:300
	Anti-CRALBP	Mouse monoclonal	%5 donkey serum in blocking solution	1:250
	Anti-HuC/HuD	Mouse monoclonal	%5 donkey serum in blocking solution	1-5 µg/ml
	Anti-Glutamine Synthetase	Rabbit polyclonal	%5 donkey serum in blocking solution	1:3000
	Anti-GFAP	Mouse monoclonal	%5 donkey serum in blocking solution	1:300
Secondary antibodies	anti-Rabbit IgG	Donkey	-	1:1000

Table 4.1. List of antibodies and their working solutions used in immunohistochemistry (cont.).

	anti-Mouse IgG	Donkey	-	1:2000

4.4. Protein Extraction from Tissue for Western Blot Analysis

Dissected retina was taken into ZR BashingBead^{TM} lysis tube containing 300 µl of cell lysis buffer with phosphatase and protease inhibitor cocktails. The tube was taken to MagNa Lyser machine and vibrated 2x60 seconds at the speed of 6500 rpm. Then, the samples were centrifuged at 4^{o}C, 12000 rpm for 30 minutes. The supernatant was collected without disturbing the pellet and they were stored separately at -80^{o}C until use.

4.5. BCA Assay

In order to determine concentration of proteins, BCA Assay kit was used. Ten-ul of BSA dilutions ranging from 0.025 to 2 mg/ml were prepared in lysis buffer and a blank solution was included. The samples were mixed with 170 µl of 50:1 diluted BCA Working Solution. Each cell lysate was diluted in lysis buffer and they were also mixed with 170 µl of 50:1 diluted BCA Working Solution. All the samples were incubated in at 37^{o}C for 30 minutes. Absorbance of all standard samples was measured at 595 nm and the standard curve was generated. The absorbance of all unknown samples was measured and concentration of each sample was extrapolated from the standard curve.

4.6. Polyacrylamide Gel Electrophoresis (SDS-PAGE)

For all the Western Blot analysis, 10% running and 5% stacking gels were prepared as follows. For 10% running gel, 2334 ul 30% Acrylamide:BisAcrylamide (37.5:1), 1.75 ml of 1.5 M Tris-Cl (pH: 8.8), 2769 µl of dH2O , 70 µl of 10% SDS, 70 µl of APS and 7 µl TEMED were mixed. The solution was poured in between 1.5 mm thick glass plates and allowed to be polymerized.

For 5% stacking gel, 500 µl of 30% Acrylamide:BisAcrylamide (37.5:1), 380 µl of 1M Tris-Cl (pH: 6.8), 2058 µl dH2O, 30 µl of 10% SDS, 30 µl of APS and 3 µl of TEMED were mixed and subsequently the solution was poured onto 10% running gel, 1.5 mm tick gel comb was placed onto stacking gel and it was allowed to be polymerized. Cell lysates in protein sample buffer were incubated at 95°C for 5 minutes to denature proteins. Lysates together with PageRuler Prestained Protein Ladder were loaded to the SDS-polyacrylamide gel. Gel was run at 80 V until sample passed the stacking gel and later on at 100 V.

4.7. Western Blot Analysis

Cell lysates containing 100 µg protein in protein sample buffer were loaded to SDS-polyacrylamide gel and the gel was run at 80 V until the loading dye passed by the stacking gel part and then at 100 V in running gel part. After gel electrophoresis, proteins were electroblotted to PVDF membrane in transfer buffer at 100 V (120 minutes for SIK2, 150 minutes for IRS1, 45 minutes for β-actin). The membrane was washed in TBS-T solution for 3x10 minutes each. The membrane was then incubated in appropriate blocking solution (Table 4.2) for 1 hour at room temperature with gentle shaking and incubated in appropriate primary antibody in desired dilutions (Table 4.2) at 4^0C overnight. The membrane was washed 3 times with TBST solution at room temperature and incubated in the mixture of Lumi-light Western blotting substrate and maximum sensitivity substrate for 1 minute. The images were captured using Stella imaging system (Raytest, Germany) (with 1-minute exposure for SIK2 and IRS1, with 5-second exposure for β-actin).

Table 4.2. List of antibodies and their working solutions used in Western Blot analysis.

	Antibody	**Brand**	**Host**	**Blocking**	**Dilution**	**Tag**
Primary antibodies	Anti-SIK2	Novus	Rabbit polyclonal	%5 MP +%1 BSA in TBST	1:2500 in %5 BSA in TBST	-
	Anti-pSer 789 IRS1	Cell Signaling	Rabbit polyclonal	%5 BSA in TBST	1:1000 in %5 BSA in TBST	-

Table 4.2. List of antibodies and their working solutions used in Western Blot analysis (cont.).

Primary antibodies	Anti-IRS1	Cell Signaling	Rabbit polyclonal	%6 MP+ %1 BSA in TBST	1:1000 in %6 MP+ %1 BSA in TBST	-
	Anti-B-actin	Santa cruz	Mouse monoclonal	%1 MP in TBST	1:5000 in %1 BSA in TBST	HRP
Secondary antibody	Anti-rabbit IgG	Santa cruz	Goat	-	1:5000	HRP

4.8. Immunoprecipitation of SIK2

The following protocol was set for immunoprecipitation of SIK2 from a single rat retina.

Fifty µl of protein A agarose beads were equilibrated with immunoprecipitaion lysis buffer containing 50 mM Tris-HCl (pH 8.0), 150 mM NaCl, 1% NP40 with phosphatase and protease inhibitor cocktails at 4^{o}C. The beads were then incubated in lysis buffer containing 1 µg/ml SIK2 antibody for 2 hours at room temperature.

For preclearance of cell lysate, 30 µl of protein A agarose beads were equilibrated with lysis buffer containing phosphatase and protease inhibitor cocktails at 4^{o}C. Washed beads were incubated with retinal lysate for 1 hour at 4^{o}C in order to eliminate nonspecific binding. The cell lysate was collected with centrifugation for 3 minutes at 4^{o}C, 13200 rpm and the beads were removed.

After preclearance, protein concentration of lysate was determined. Incubated antibody&beads complex was mixed with 750 µg of protein lysate and incubated overnight. The beads were collected with centrifugation for 3 minutes at 4^{o}C, 13200 rpm.

Beads were washed 3 times at 4^{o}C. Three fifth of the slurry beads in lysis buffer was taken for IVK Assay while the rest was used in Western Blot analysis.

For the Western Blot analysis, 20 µl of SIK2 containing beads were mixed with equal volume of 2X SDS sample buffer and they were incubated at 95^{o}C for 5 minutes. Then they were centrifuged at 4^{o}C for 5 minutes and the supernatant was taken to load to the gel. The rest procedure was carried on as indicated in Section 4.7.

4.9. SIK2 and IRS1 Co-Immunoprecipitation

SIK2 immunoprecipitation from retinal cell lysate was performed (Section 4.8) except with Co-IP lysis buffer containing 20 mM Tris-HCL (pH:7.5), 150 mM NaCL, 1 mM EDTA, %1 Triton-X with phosphatase and protease inhibitor cocktails. For 500 µg of total protein, 50 µl of protein A agarose beads and 1 µl anti-SIK2 antibody were used. Western Blot was carried on as described in Section 4.7. Anti-SIK2 and anti-IRS1 antibodies were used as specified in Table 4.2 for the detection of the proteins.

4.10. In Vitro Kinase Assay

The kinase activity of SIK2 was monitored through changes in autophosphorylation levels by using non-radioactive phosphatase-coupled Universal Kinase Activity Kit (RnD Systems). One mM ADP, 1 mM ATP and 10 ng/µl Coupling Phosphatase 4 in Phosphatase Buffer were prepared freshly in requested amounts as instructed by manufacturer.

4.10.1. Phosphate Standard Curve Determination

Serial dilutions of Phosphate Standard provided by the kit were prepared in Assay Buffer. 50 µl of each dilution was transferred into 96-well microplate in duplicate. 30 µl of Malachite Green Reagent A, 100 µl of distilled water and 30 µl of Malachite Green Reagent B were sequentially added to the wells and the samples were mixed by tapping the plate gently. The plate was then incubated for 20 minutes at room temperature to stabilize the color development. The OD of each well was determined using microplate reader set to 620 nm. The average of duplicate readings were evaluated and the OD of the average

blank standard was subtracted. Finally the plot of the phosphate input (pmol) vs. the corrected OD was generated and an equation was extracted (e.g. $y = 4524{,}4x - 67{,}873$). x in the equation corresponds to OD while y is phosphate.

4.10.2. Kinase Assay Protocol

Thirty-µl of SIK2 immunoprecipitated as described in Section 4.8 was mixed with 10 ul of 10 ng/µl Coupling Phosphatase 4. For negative control, 10 µl of 10 ng/µl Coupling Phosphatase 4 was added to 30 µl of Assay Buffer; and for positive control, 10 µl of Coupling Phosphatase 4 was added to 30 µl of immunoprecipitated SIK2. 50 µl of Assay Buffer was used as an assay blank. In the final step, 10 µl of 1mM ATP was added to each sample except positive control and blank sample. 10 µl of 1mM ADP in place of ATP was added to positive control. Addition of ATP and ADP initiated the reaction and the microplate was incubated for 30 minutes at room temperature. The plate was tapped gently every 5 minutes. At the end of 30 minutes, the reaction was terminated by adding 30 µl of Malachite Green Reagent A to each well. The samples were mixed by tapping the plate gently. 100 µl of distilled water and 30 µl of Malachite Green Reagent B were sequentially added to each well. The microplate was incubated for 20 minutes at room temperature by tapping the plate every 5 minutes. After incubation, the OD of each well was determined using the microplate reader set to 620 nm and the OD values were adjusted by subtracting the OD of the blank solution. The phosphate amount of each kinase reaction was calculated using the previously determined standard curve equation.

4.11. Statistical Analysis

A two-tail paired Student's t-test was performed between experimental and control groups for statistical analysis. Means with $P < 0.05$ were considered statistically significant.

5. RESULTS

5.1. Diabetes Induction in Wistar Albino Rats

In order to analyze whether SIK2 contributes to the progression of DR, diabetic animal model was generated with a single dose of STZ injection to male Wistar Albino rats. STZ is specifically toxic to insulin producing pancreatic β cells (Wei *et al*., 2003).

The rats (250-350 gr) were injected once with STZ in citrate buffer intravenously, while control rats were injected with citrate buffer alone. The fasting blood glucose levels were measured two days later and the animals with higher than 200 mg/dl blood glucose levels were considered diabetic. All animals were fed with normal diet until they were sacrificed at day 0, 2 weeks, 4 weeks and 8 weeks post-injection.

The fasted blood glucose levels and weights of the experimental and control rats of each group were measured once a week until the day of sacrifice. While fasted blood glucose levels of control rats remained unchanged, the average fasted blood glucose levels of diabetic rats increased gradually throughout the duration of the experiment (Figure 5.1a). The rats in the diabetic groups lost significant weight compared to the control animals, and weight loss gradually increased in time as expected (Figure 5.1b).

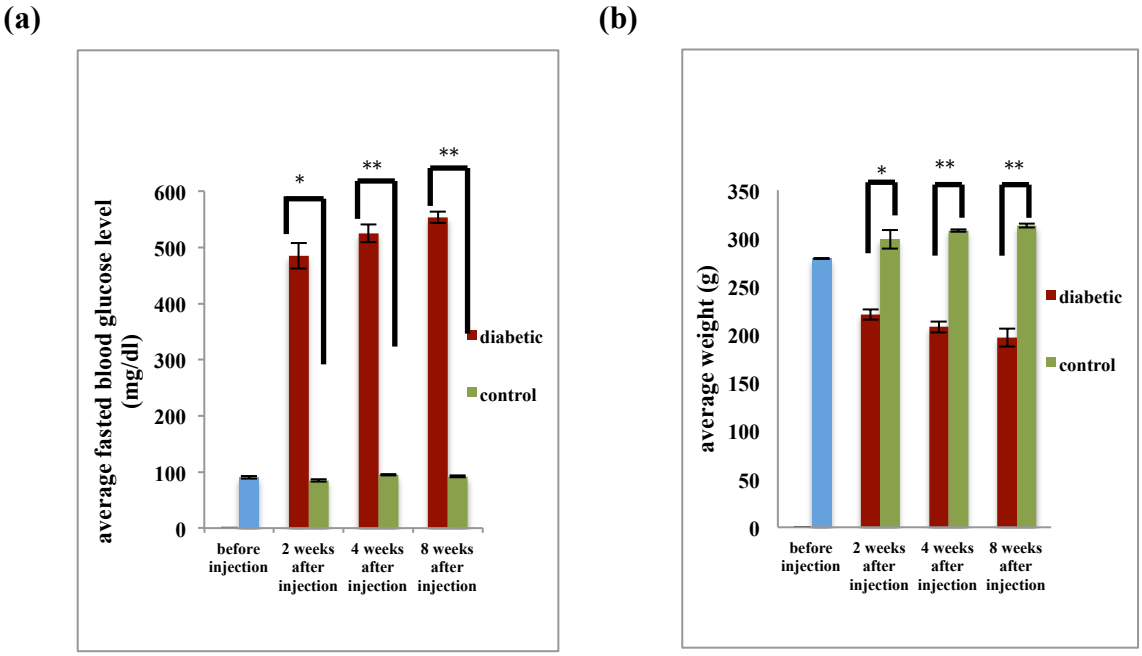

Figure 5.1. Changes in the fasting blood glucose levels and weights of rats. The animals in the experimental group received STZ and the control group received vehicle injections, (a) average fasted blood glucose levels and (b) average weights of the animals monitored ($n \geq 5$ animals were used per timepoint. *:$p \leq 0.05$, **:$p \leq 0.001$)

5.2. Effect of Hyperglycemia in Rat Retina

One of the very early events that take place in the retina in response to pathological alterations such as hyperglycemia is Müller cell gliosis (Bringmann *et al*., 2006). In order to confirm that Müller cells undergo gliosis in response to hyperglycemia, the retinal tissues of diabetic and control rats from each group were excised and the sections were double-labeled with the antibodies for GFAP, gliosis marker, and GS, a Müller cell specific enzyme. GFAP normally is not expressed in healthy adult retina and upregulation of GFAP in Müller cells is considered to be the cellular marker for the alterations in Müller cell function.

The results showed that GFAP signal was undetectable in control rat retina, while in diabetic retina expression of GFAP was upregulated starting from Müller cell end-feet located in GCL as early as the 2nd week of diabetes (Figure 5.2). Thereafter, GFAP expression was further enhanced and extended from the GCL through the ONL along the entire length of Müller cells throughout the retina compared to controls (Figure 5.2).

Contrary to GFAP upregulation, GS expression was decreased within 8-week of diabetes onset, supporting the changes in Müller cells and loss of Müller cell function. The signal observed in outer retina above photoreceptor layer is the autofluorescence of rhodopsins found in Retinal Pigment Epithelium (RPE) (Katz *et al*., 1989). In conclusion, these data confirms that Müller cells undergo reactive changes and show signs of gliosis even in the early phases of diabetes.

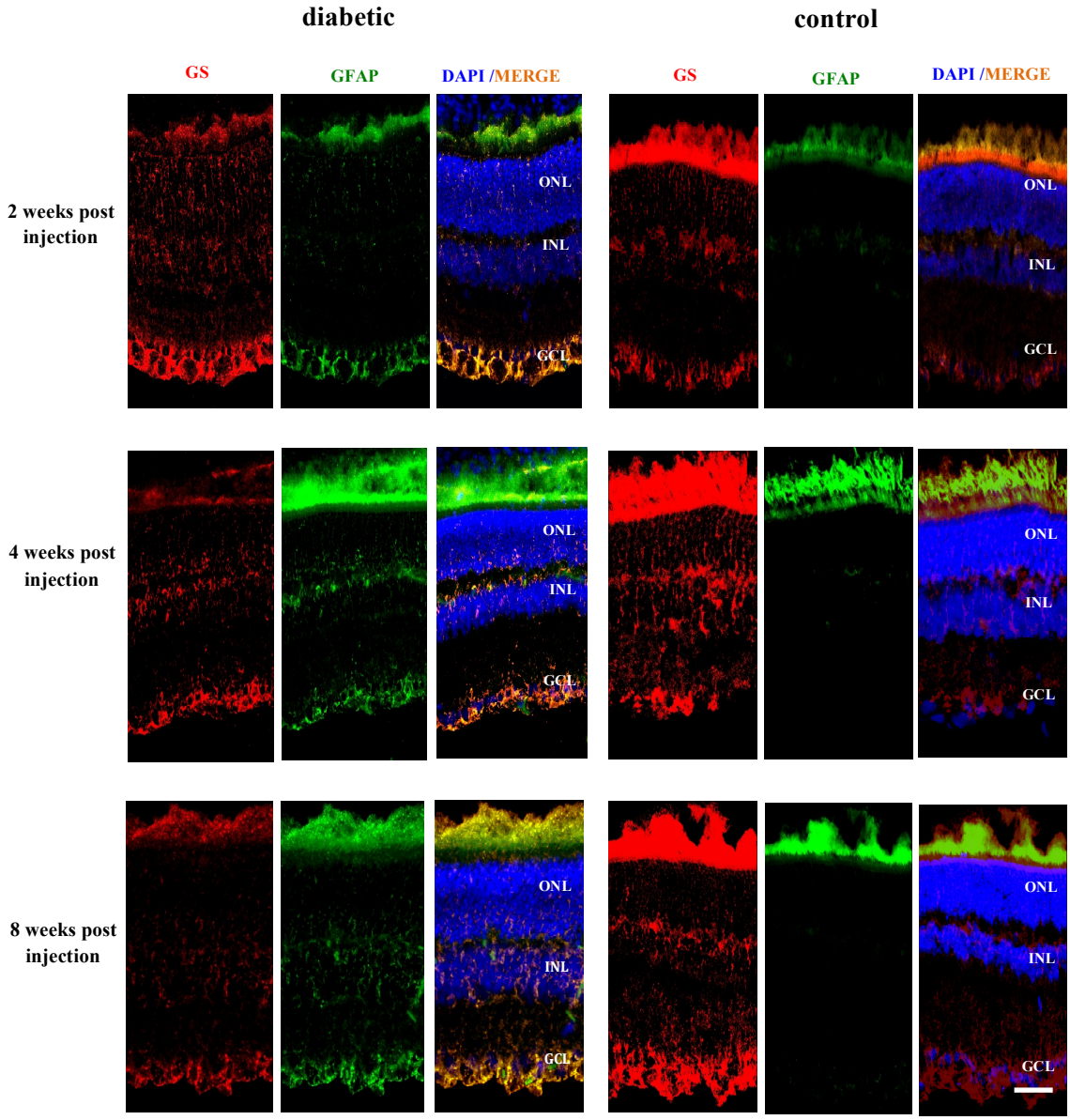

Figure 5.2. Gliosis in diabetic retina. Sections of 2, 4 and 8-week diabetic and control rat retinal tissues were stained with Müller cell marker GS (red), gliosis marker GFAP (green) and DAPI (blue). Scale bar: 50 μm for all panels.

It is known that retinal cell death occurs by apoptosis during diabetes. It has been reported that in STZ-induced hyperglycemia, the number of apoptotic cells in the retina increases as early as 3-4 weeks after the induction of diabetes (Barber *et al*., 1998; Oshitari *et al*., 2005). In order to construct a time profile for cell death analysis in DR, cryosections of retinae from rats sacrificed 2, 4 and 8 weeks after the onset of diabetes and the age-matched control sections were stained with the antibody for apoptosis marker, cleaved Caspase 3. The results indicate that no cell death was detectable within 2 weeks of diabetes (Figure 5.3). In the 4-week diabetic retina, even though no apoptotic cells was observed in INL and photoreceptor layer (ONL), some cells in GCL were positive for cleaved Caspase 3. Double-labeling with HuC/HuD, a ganglion cell marker, and cleaved Caspase 3 showed that these apoptotic cells were indeed ganglion cells (Figure 5.4).

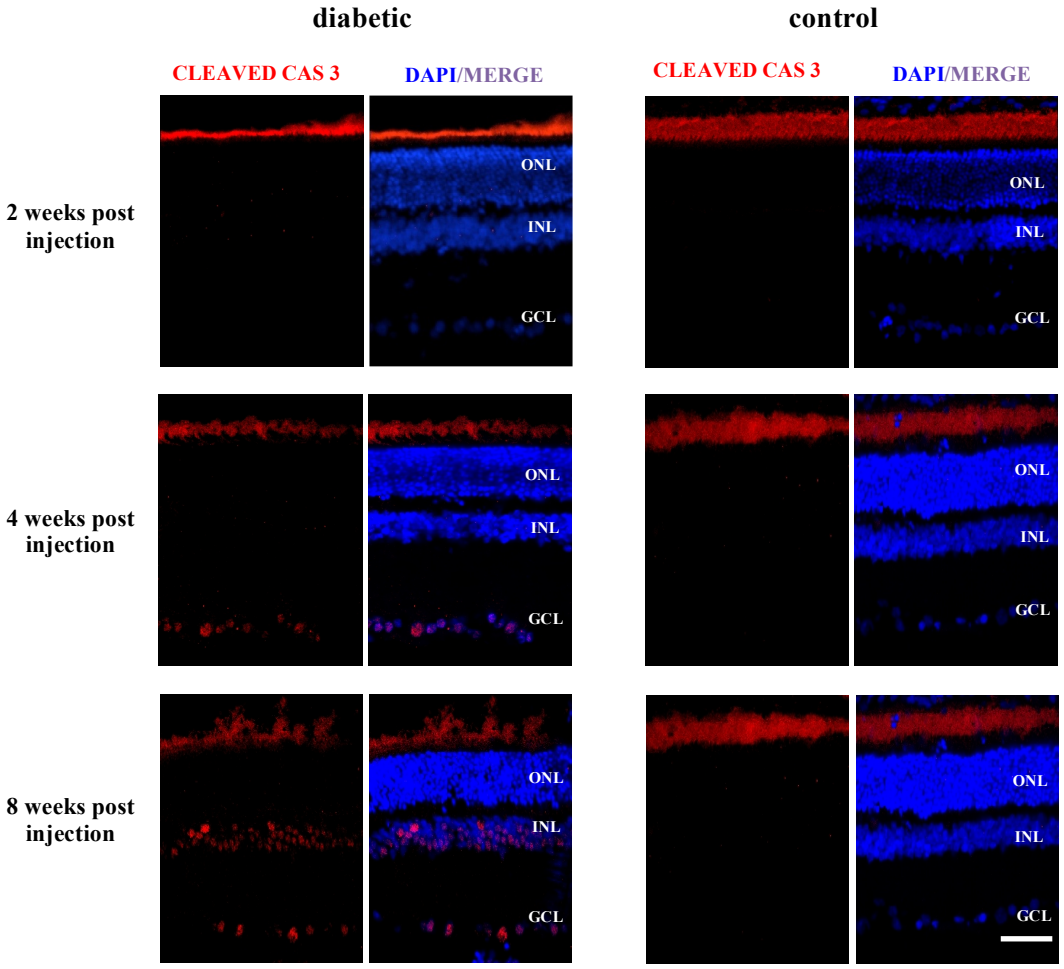

Figure 5.3. Cell death in diabetic retinae. Sections of 2, 4 and 8-week diabetic and control rat retinal tissues were stained with the apoptosis marker cleaved Caspase 3 (red) and DAPI (blue). Scale bar: 50 μm for all panels.

Cell death in INL became apparent by 8-weeks after the onset of hyperglycemia (Figure 5.3). Eight-week diabetic rat retina was stained with CRALBP, Müller cell marker, and cleaved Caspase 3 (Figure 5.5). The presence of double-positive cells in INL as shown with white arrowhead confirmed Müller cell death (Figure 5.5a). Müller cells are regularly aligned in the middle of the INL in normal retina (Jayaguru et al., 2011). However, in the diabetic rat retina, we observed that some Müller cell bodies were displaced as shown in Figure 5.5b with blue arrowheads, which is considered to be another indicator of downregulation of Müller cell function (Jayaguru et al., 2011). The presence of cleaved Caspase 3-positive CRALBP-negative cells as shown in Figure 5.5a with yellow arrowhead suggested that neurons in INL died as well within this time frame of diabetes.

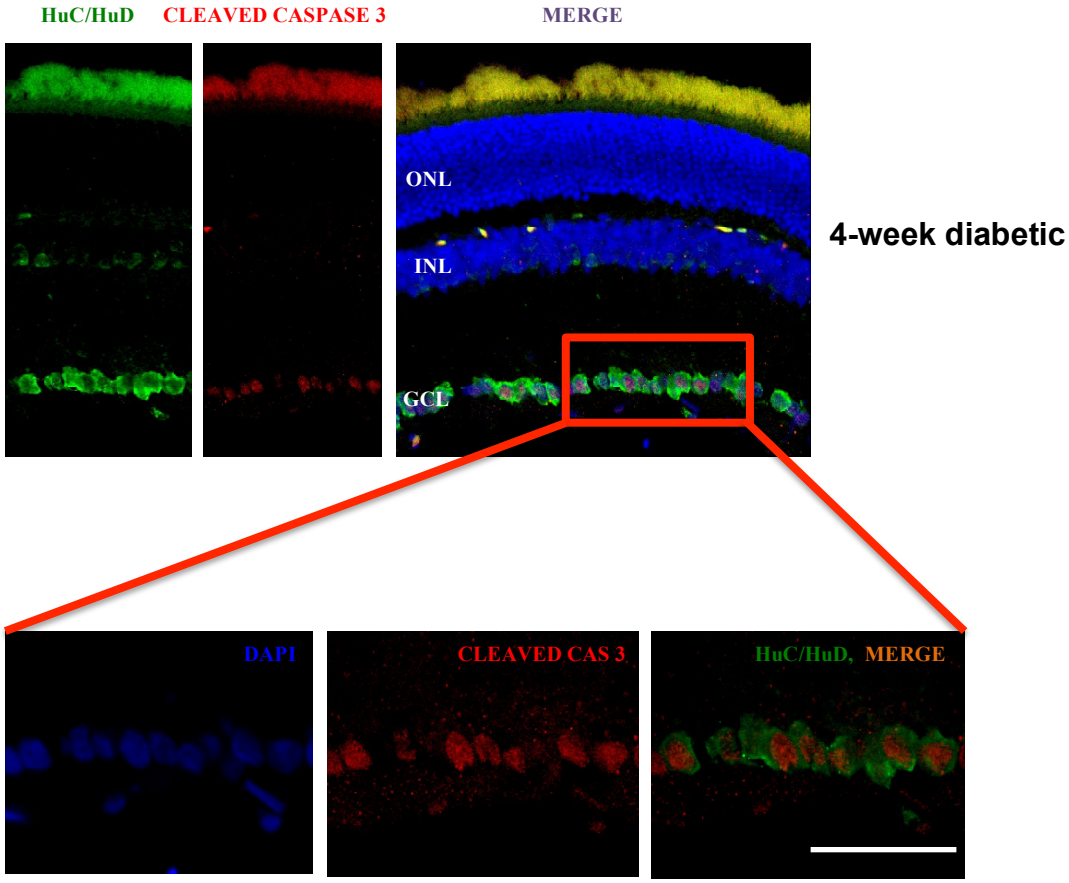

Figure 5.4. Apoptosis in ganglion cells. 4-week diabetic rat retina was stained with anti- HuC/HuD (green), ganglion cell marker, anti-cleaved Caspase 3 (red) and DAPI (blue). Scale bar: 50 μm for all panels.

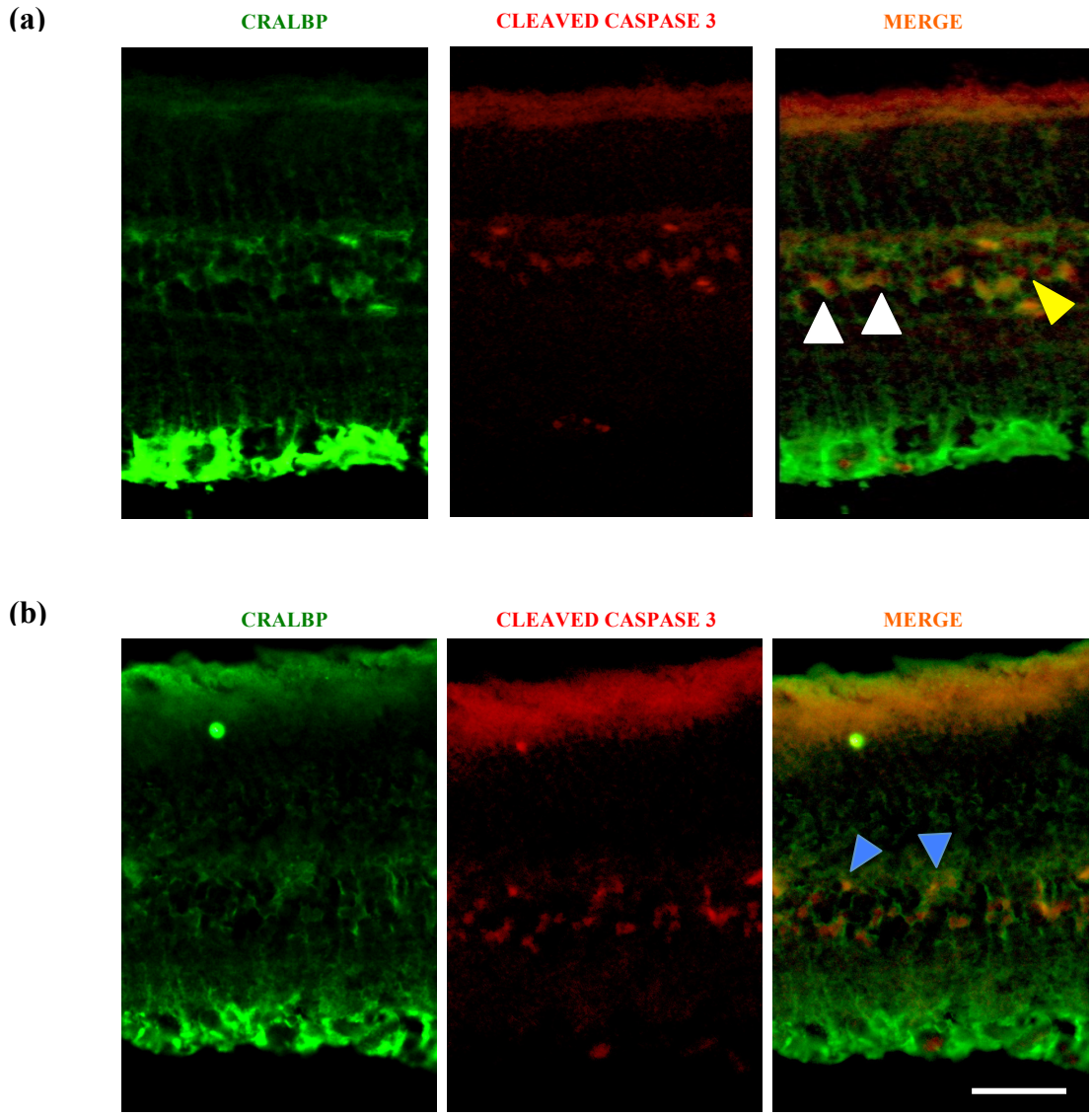

Figure 5.5. Apoptosis in Müller cells and neurons of INL. 8-week diabetic rat retinal sections were stained with anti-CRALBP (green), Müller cell marker and anti-Cleaved Caspase 3 (red). (a) White arrowheads: cleaved Caspase 3 and CRALBP + cells, yellow arrowhead: cleaved Caspase 3+ CRALBP- cells, (b) blue arrowheads: displaced Müller cell. Scale bar: 50 μm for all panels.

In conclusion, the data obtained from these immunohistochemical stainings confirms that cell death was first observed in ganglion cells in the 4th week of diabetes. With the progression of the disease, Müller cells and neurons in INL began to die in the 8th week of diabetes. However, no apoptotic cell was observed in ONL suggesting that hyperglycemia do not involve photoreceptor death within the first 8 weeks of diabetes.

5.3. The Potential Role of SIK2 in the Insulin-Induced PI3K/Akt/Survival Pathway

It is widely accepted that insulin primarily acts as a survival factor, rather than regulator of glucose metabolism in vertebrate retina (Reiter et al., 2003). It has been reported that IR activity and the PI3K-Akt-survival pathway are impaired in diabetes (Taniguchi et al., 2006; Boura-Halfon and Zick, 2009). Previous findings suggest that SIK2 is involved in the negative regulation of insulin dependent Müller cell survival *in vitro* (Küser-Abalı et al., 2013), thus we hypothesized that it may also take part in the progression of DR.

In the initial experiments, we studied whether SIK2 protein level and expression pattern changed between 2-week, 4-week, 8-week diabetic and the age-matched control retinae. Then, we analyzed modulation of SIK2 kinase activity and SIK2-IRS1 interaction within this time frame.

5.3.1. Modulation of SIK2 Protein Level in Diabetic Retinopathy

In order to follow possible changes of SIK2 protein level in the retina during the first 8-week course of diabetes, lysates of day 0, 2-week, 4-week, 8-week diabetic and the age-matched control rat retinae were subjected to Western Blot analysis (Figure 5.6a). The graph represents the average mean value of SIK2 band intensities normalized to that of β-actin in 5 independent experiments. The results indicated that SIK2 protein levels in the retina of diabetic and healthy rats did not change significantly during this time frame.

Immunohistochemical stainings of the retinal sections were performed with anti-SIK2 antibody (Figure 5.6b). The results demonstrated that SIK2 was strongly expressed in the cell bodies in INL and GCL and the expression pattern did not change between diabetic and control samples. Thus, we can conclude that retinal SIK2 levels do not change in response to hyperglycemia during early phase of diabetes.

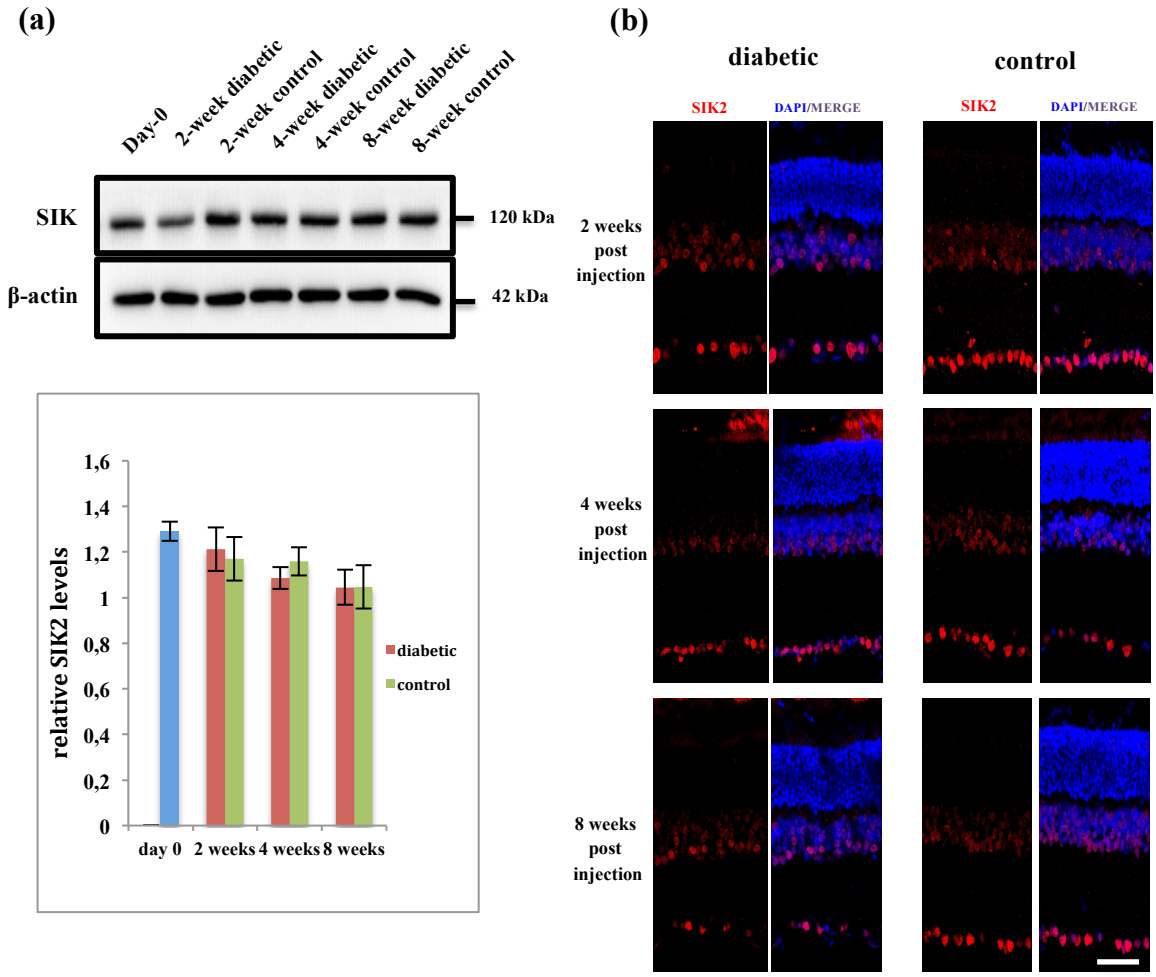

Figure 5.6. Expression of SIK2 in diabetic and control rat retina. (a) Western Blot analysis of diabetic and control retinal lysates was performed using anti-SIK2 and anti-β-actin. The graph represents the average SIK2 band intensities normalized to that of β-actin levels of the same samples. (b) Retinal sections from diabetic and control samples were stained with anti-SIK2 (red) and DAPI (blue). Scale bar: 50 μm for all panels.

5.3.2. Modulation of SIK2 Activity in Diabetic Retinopathy

Potential modulations of SIK2 kinase activity were monitored through changes in autophosphorylation levels. Non-radioactive phosphatase-coupled Universal Kinase Activity Kit (RnD Systems) was used and a standard curve was generated as instructed by the manufacturer (Figure 5.7). SIK2, like any other kinase, converts ATP to ADP while phosphorylating its substrate. The coupling phosphatase in the kit, CD39L2, releases one inorganic phosphate from ADP and free phosphates are detected with malachite green phosphate detection reagents in the kit. Therefore, the amount of released phosphate

reflects the level of kinase activity of SIK2. The equation ($y = 4524{,}4x - 67{,}873$) was extracted from the standard curve. x in the equation corresponds to OD while y is phosphate.

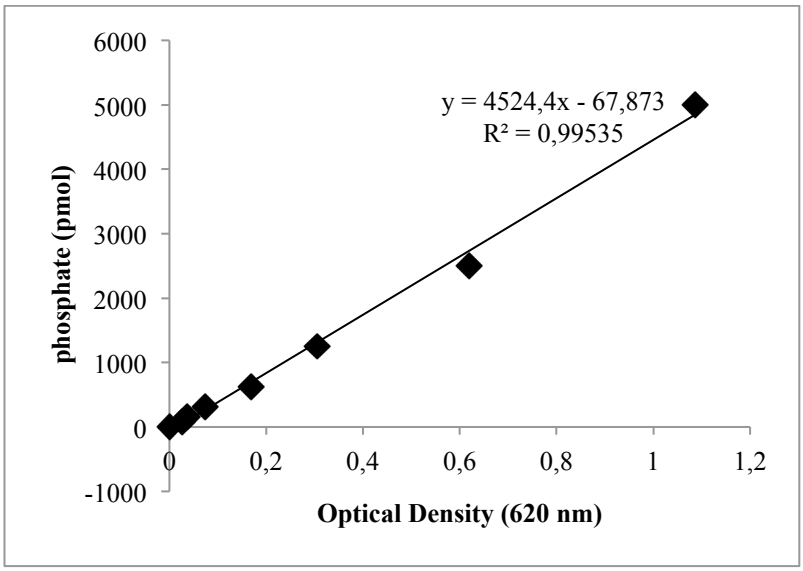

Figure 5.7. Standard curve for the kinase assay. The ODs of phosphate standards prepared in 2-fold serial dilutions were measured at 620 nm. The slope of the linear regression line (4524,4 pmol/OD in this standard curve) represents the amount of phosphate corresponding to a unit of absorbance at 620 nm.

Before carrying out experiments to determine potential changes of SIK2 activity in diabetic retina, we first determined the starting amount of protein lysate for sufficient SIK2 IP to get significant autophosphorylation measurements. Therefore, kinase assays were performed with SIK2 immunoprecipitated from 250 µg, 500 µg, 750 µg and 1000 µg of total protein lysates (Figure 5.8) The released phosphate levels of negative and positive controls were measured as 425,3 pmol and 4036,2 pmol, respectively. Since SIK2 immunoprecipitated from 250 µg of protein lysate yielded free phosphate level of 865,7 pmol that was close to negative control, we chose to use 500 µg of protein lysate for SIK2 IP in order to get a sufficient kinase activity to make a reliable comparison in kinase assays.

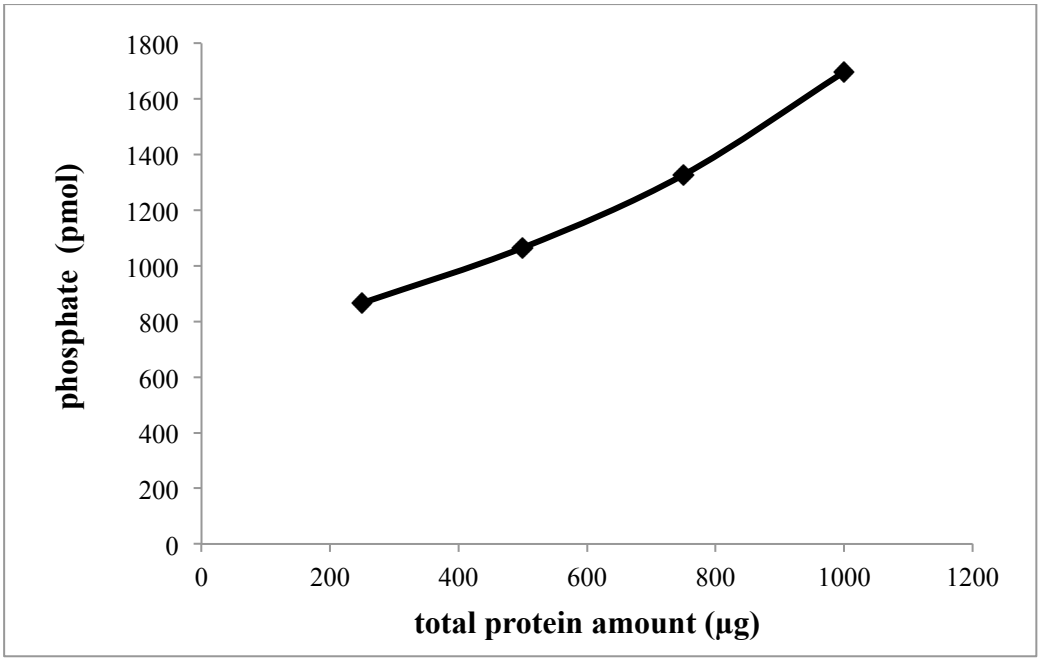

Figure 5.8. Changes in kinase activity with increasing amount of SIK2. SIK2 immunoprecipitated from 250 µg, 500 µg, 750 µg and 1000 µg of retinal lysate was used in *in vitro* kinase assay. SIK2 protein was assayed with ATP and Coupling phosphatase (CD39L2) for 30 minutes at room temperature to measure autophosphorylation activity.

To follow the modulation of SIK2 activity in retina under hyperglycemic conditions *in vivo*, the immunoprecipitated SIK2 from diabetic and the age-matched control retinae were assayed in the presence of ATP and the Coupling Phosphatase (CD39L2) for 30 minutes at room temperature. The kinase assay was performed with 4 independent sets of retinal SIK2. The OD^{620} measurement of each kinase reaction was taken and the concentration of released phosphate for each kinase assay was calculated by using the standard curve equation given in Figure 5.7 (e.g. $y = 4524{,}4x - 67{,}873$). The ratio of released phosphate to immunoprecipitated SIK2 band intensity reflects the kinase activity.

The results indicated that SIK2 activity in 2-week diabetic retina seemed to be greater than the control (Figure 5.9). Although the increase was not as much as in the 2-week diabetic retina, there seemed to be a higher SIK2 activity in 4-week diabetic retina compared to its control. However, no difference was detectable in SIK2 activity between 8-week diabetic and control retina.

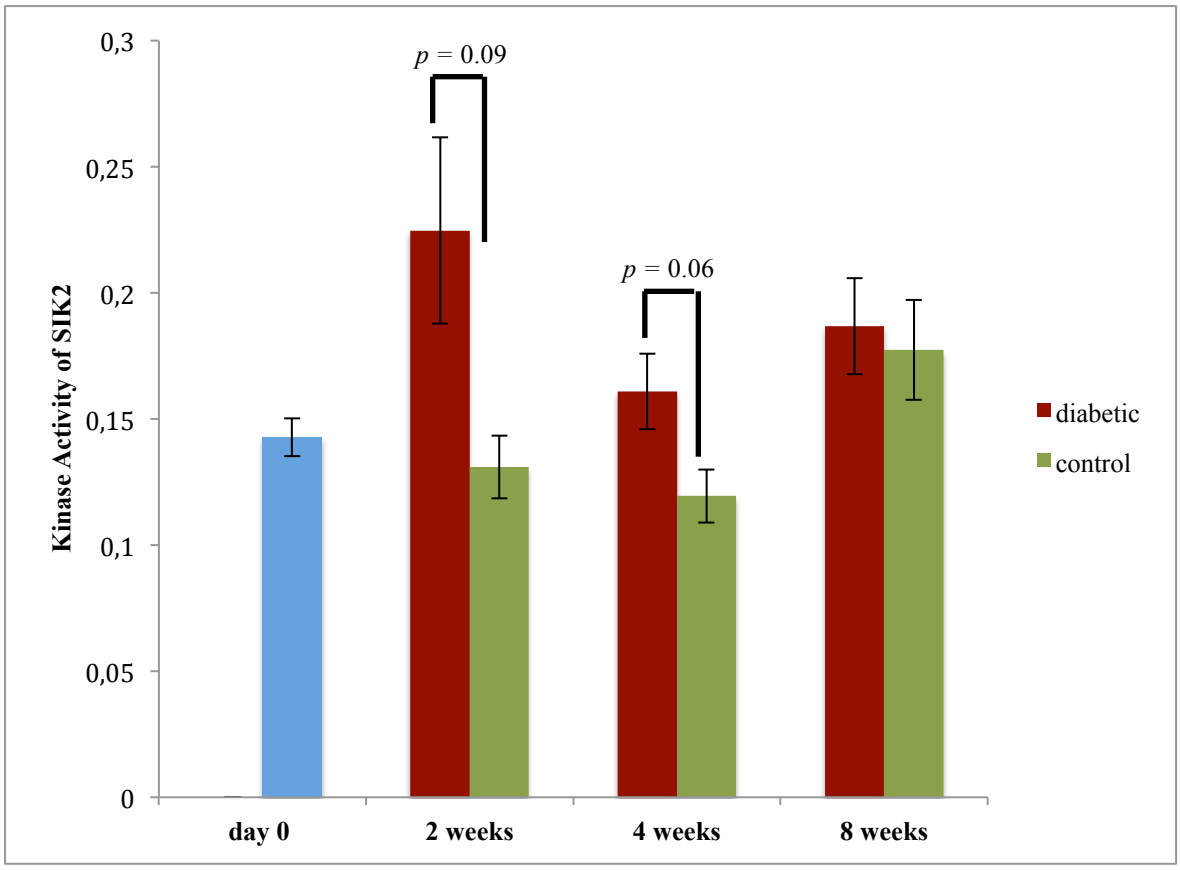

Figure 5.9. Changes in SIK2 activity in hyperglycemia. SIK2 immunoprecipitated from day 0, 2-week, 4-week, 8-week and age-matched control rat retina was used in *in vitro* kinase assays. The bars represent the released phosphate amount from each assay normalized to SIK2 protein level in the same samples. ($n = 4$ animals were used per each condition).

5.3.3. Modulation of SIK2-IRS1 Interaction in Diabetic Retinopathy

The docking protein IRS1 plays a critical role in regulation of insulin signaling (Boura-Halfon and Zick, 2009) and SIK2 acts as an upstream kinase of IRS1 and targets S789 (Horike *et al*., 2003). It has been previously shown by our group that SIK2 acts as a negative modulator of the insulin-dependent survival pathway in Müller cells via IRS1 serine phosphorylation *in vitro* (Küser-Abalı et al., 2013). Therefore we investigated whether SIK2-IRS1 interaction in the retina was modulated by hyperglycemia by performing co-IP studies.

The SIK2 immunoprecipitates from the lysates of day 0, 2-week, 4-week, 8-week

diabetic retinae and the age-matched control retinae were subjected to immunoblot analysis with anti-IRS1 and anti-SIK2 antibodies (Figure 5.10a), and the IRS1 band intensities were normalized to that of SIK2 in the same sample. The result suggests that SIK2 and IRS1 directly interact in the retina and this interaction is enhanced by hyperglycemia beginning from the 4^{th} week of STZ injection (Figure 5.10b).

In conclusion, it can be suggested that although SIK2 protein levels do not show a change, its activity in the retina seems to be upregulated to a limited extend upon hyperglycemia as early as 2 weeks after diabetes induction consistent with the earlier report (Küser-Abalı et al., 2003). It is conceivable that the enhanced SIK2-IRS1 interaction reflects negative regulation of IRS1 by SIK2 under hyperglycemic conditions. Thus, inactivation IRS1 by SIK2 together with other known upstream kinases may provoke the impairment of insulin-induced survival pathway, consequently contributing to cell death.

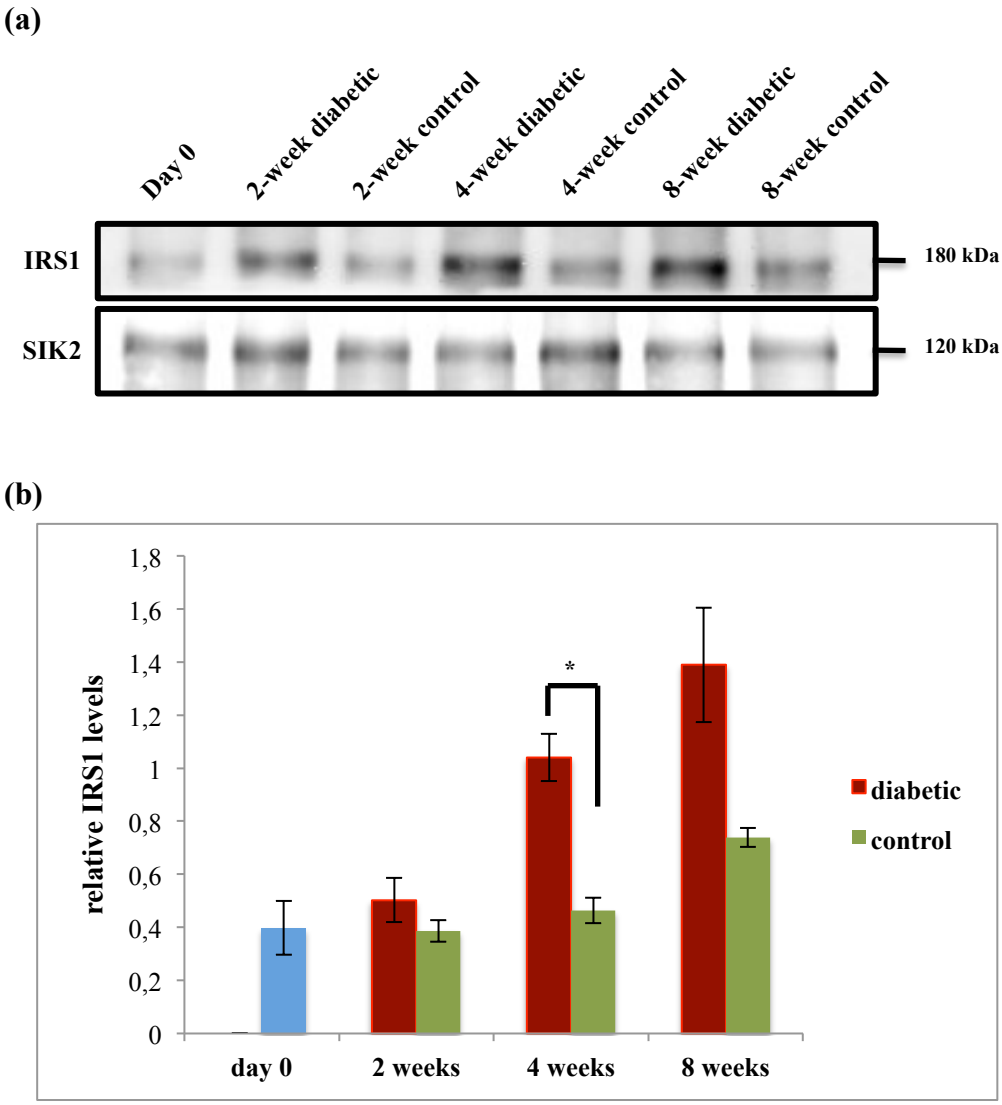

Figure 5.10. SIK2 co-immunoprecipitation with IRS1. (a) SIK2 immunoprecipitates obtained from the lysates of 2-week, 4-week, 8-week diabetic and the age-matched control retinae were analyzed by Western blotting with anti-SIK2 and anti-IRS1 antibodies. (b) The graphic represents the average of IRS1 band intensities normalized to that of SIK2 levels in the same samples ($n = 3$ animals were used per each condition, *:$p \leq 0.05$).

6. DISCUSSION

It has been reported that SIK2 expression is upregulated in white adipose tissue of db/db diabetic mice (Horike *et al*., 2003). In the same study it was shown that in mouse adipocytes SIK2 phosphorylates and downregulates IRS1, which is an important regulator of insulin pathway, suggesting that SIK2 might be involved in insulin resistance. Recent findings indicated that SIK2 activity on IRS1 increased while basal levels of pAkt (S473) decreased in cultured Müller glia cells grown under chronic hyperglycemia (Küser-Abalı *et al*., 2013). Moreover SIK2 overexpression under normoglycemia mimics the chronic hyperglycemia condition and accelerates cell death *in vitro* (Küser-Abalı *et al*., 2013). Taken together, it has been suggested that there is a negative correlation between SIK2 activity and insulin signaling to promote cell survival in Müller cells. In this context, we aimed to identify the potential involvement of the serine/threonine kinase SIK2 in STZ induced DR.

The glucose analog STZ is widely used to induce experimental diabetes in animals because of its relatively specific cytotoxic effect on insulin producing pancreatic β-cells (Schnedl *et al*., 1994). The loss of insulin producing cells results in decrease in systemic insulin level and increase in blood glucose mimicking Type 1 diabetic state. Studies have shown that a single dose of STZ injection is sufficient to generate diabetic rats that exhibit many of the symptoms of chronic human diabetes including DR (Wei *et al*., 2003). In the course of our study, experimental rats were injected with 60 mg/kg STZ solubilized in citrate buffer intravenously once while control rats received vehicle injections. The excess water consumption and urination in diabetic rats taken together with the increased fasted blood glucose level and decreased body weight profiles indicate that we successfully generated diabetic rats.

One of the most common complications of diabetes is the development of DR that involves gliosis, degeneration of retinal neurons and vascular abnormalities, which may eventually lead to vision loss (Barber *et al*., 2005; Miyamoto *et al*., 1999). In neuronal tissues insulin acts as a growth factor rather than a metabolic regulator and participates in development, differentiation, growth and survival processes (Reiter *et al*., 2003). One of

the very early events that take place in the retina in response to disease and injury states is Müller cell gliosis where several functions of Müller cell are altered (Bringmann *et al*., 2001; Bringmann *et al*., 2006). The upregulation of intermediate filament GFAP in Müller cells is considered to be a highly sensitive indicator of gliosis in diseased retina (Bringmann *et al*., 2006). In our study, we followed changes in GFAP expression in diabetic and control retina to monitor the progression of gliosis throughout the first 8-weeks of diabetes. The upregulation in GFAP expression in the diabetic retina was apparent by the 2nd week of diabetes starting from Müller cell end feet. By the 4th week of the diabetes, GFAP signal spanned the retina from the inner retina (GCL) to the outer membrane along the entire length of the Müller cells. Although the exact function of GFAP remains poorly understood, it is known to play a role in glia-neuron interaction and its upregulation in the retina is the indicator of glial scar formation which suggests the abnormal structure of Müller cells (Weinstein *et al*., 1991).

GS, a Müller cell-specific enzyme, is involved in recycling of the neurotransmitter glutamate and the prevention of glutamate accumulation in the retina (Bringmann *et al*., 2006). Decrease in GS expression results in increased retinal glutamate leading to alteration in synaptic function and potentially causing neurodegeneration via NMDA-receptor mediated excitotoxicity (Lieth *et al*., 2000). Although there is a study indicating that no change in GS expression was observed in diabetic retinae obtained from postmortem human donors (Mizutani *et al*., 1998), it has been reported that in Müller cells cultured from neonate rat retinae, high glucose decreases GS expression (Shen *et al*., 2010). The immunohistochemical stainings in our study showed that in contrast to GFAP, GS expression decreased gradually in the same time frame of diabetes. At this time it is not clear whether decreased GS signal results from Müller cell death or decreased expression *per se*. At any rate taken together, the gradual increase in GFAP immunoreactivity and gradual decrease of GS labeling in diabetic rat retina suggest that Müller cells show signs of change starting from the 2nd week of diabetes and it can lead to the impairment of Müller cell supportive functions on the survival and neuron function.

It has been reported that in STZ-induced hyperglycemia, accelerated apoptosis of retinal neurons and glial cells starts as early as 4 weeks after the induction of diabetes in rats and a similar increase was noted in 6-year diabetic human retina (Barber *et al*., 1998;

Oshitari *et al*., 2005). The decrease in ganglion cell population is estimated to be about 15% after 4 weeks and 20% after 4 months of STZ injection compared with the age-matched control rats suggesting that the apoptotic cells are likely to include ganglion cells early in diabetes (Zeng *et al*., 2000). In 4 month-diabetic rats, the number of apoptotic neurons in the INL increase by more than 50% (Zeng *et al*., 2000). Although there is a study showing that loss of Müller cells in the diabetic rat retina was observed within 4 months after induction of diabetes, there is still lack of information about the faith of Müller cells in the early time frame of diabetes (Jayaguru *et al*., 2011). On the other hand, the apoptotic photoreceptor cells have been shown to be rare in the early phases of diabetes but remarkable in 12-week and 24-week diabetic retinas suggesting that photoreceptors can be the last affected cell type by diabetes in the retina (Park *et al*., 2003). The cell death profile of photoreceptors, amacrine, bipolar and horizontal cells of the retina early in diabetes awaits further investigation.

To better define the progression of apoptosis in our DR model, retinal sections of the 2-week, 4-week, 8-week diabetic and the age-matched control rats were probed for apoptosis marker cleaved Caspase 3. In accordance with the earlier studies, GCL death was first observed by 4 weeks after the onset of diabetes, and apoptosis in INL cells were observable by 8 weeks, but no cell death was detectable in ONL within this time frame. Although almost all the cells in GCL are expected to be ganglion cells, sometimes displaced amacrine cells can be found in GCL (Centanin and Wittbrodt. 2014). Therefore, an effort to characterize apoptotic cells in GCL was made by double labeling of 4-week diabetic retina with ganglion cell marker HuC/HuD and cleaved Caspase 3. The presence of double positive cell bodies located in GCL proved that all these apoptotic cells were indeed ganglion cells.

Increase in apoptosis of cultured Müller glia cells grown under chronic hyperglycemia was shown by our group previously (Küser-Abalı *et al*., 2013). To demonstrate that Müller cell death also occurs *in vivo*, we carried out double staining of retinal sections with Müller cell marker anti-CRALBP and anti-cleaved Caspase 3 in 8-week diabetic rat retina. The presence of double-positive cells and also cleaved Caspase 3-positive CRALBP-negative cells in INL showed that both Müller cells and neurons undergo apoptosis in this time frame of diabetes. In healthy retina, Müller cells are known

to be regularly aligned in the middle of the INL. There is a study suggesting that the regular order of Müller cells was disrupted in the diabetic retina and those cells were shown to be more likely apoptotic than the regularly aligned cells (Jayaguru *et al*., 2011). In our study it was also evident that the a few Müller cells were displaced in diabetic retina concurrent with this earlier report (Jayaguru *et al*., 2011).

Based on this data, it can be suggested that apoptosis of the neurons and Müller cells begin following the onset of gliosis. It is evident that the both events are initiated at innermost part of the retina, which is GCL, and progressed through INL. It encourages us to speculate that apart from the failure of insulin-induced PI3K/Akt/survival pathway, gliosis progression itself by the impairment of supportive functions of Müller cells may have an additive effect on the loss of retinal cells, by raising the susceptibility of neurons to stressful stimuli in the diabetic retina.

We next focused on the possible involvement of the SIK2 in insulin-dependent survival pathway in the retina. Binding of insulin to its receptor triggers phosphorylation of Tyr residues of IRS1 (Sun *et al*., 1993) that in turn results in specific and strong association between IRS1 and PI3K, forming a docking site for them at the membrane (Madonna *et al*., 2012). Conversion of PIP2 into PIP3 by PI3K activates PDK1 and recruits Akt to the membrane (Vivanco *et al*., 2002). Then PDK1 and mTOR/Rictor complex mediate the phosphorylation and activation of Akt (Dummler *et al*., 2007). It has been reported that in cultured Müller cells, Akt activation via Tyr-phosphorylation of IRS1 evokes insulin-induced survival responses but the regulation of the pathway is ill defined (Gosbell *et al*., 2000; Ola *et al*., 2011). On the other hand, insulin-stimulated Ser/Thr phosphorylation of IRS1 evokes a negative feedback mechanism by blocking the Tyr phosphorylation sites and inducing the dissociation of IRS1 from the insulin receptor and intracellular complexes (Mothe *et al*., 1996). It has been also reported that Ser/Thr phosphorylation of IRS1 triggers degradation of the protein in adipocytes under hyperglycemia (Pederson *et al*., 2001). Thus SIK2, as one of the kinases that are responsible for serine phosphorylation of IRS1 (Horike *et al*., 2003), might be involved in insulin resistance via alterations of its expression and activity level in a mutually non-exclusive manner.

A recent study of our group showed that in cultured Müller glia both SIK2 expression and activity increased while pAkt level decreased when the cells were exposed to high glucose suggesting that SIK2 could be involved in the impairment of survival (Küser-Abalı *et al*., 2013). This finding raises the possibility that *in vivo* SIK2 levels/activity in hyperglycemia may also be enhanced and negatively regulate insulin-dependent survival pathway. Since SIK2 acts as one of the upstream kinases of IRS1 and Akt in insulin-induced survival pathway in cultured Müller cells (Küser-Abalı *et al*., 2013), it is highly possible that it may interfere in the pathway before the cell death begins. For the clarification of SIK2 involvement in the progression of the disease, we analyzed SIK2 in the early phases of DR including the first 2 weeks of diabetes, in which cell death was not observed yet. As a first step towards better understanding of SIK2 involvement in the negative regulation of survival pathway, we first investigated whether SIK2 protein levels changed in diabetic retinae by Western Blot analysis. The results showed that SIK2 expression in the retina did not change during the first 8-weeks of diabetes, that was contrary to the finding that SIK2 expression increased in cultured Müller glia grown under chronic hyperglycemia (Küser-Abalı *et al*., 2013). Based on this finding, one would expect that SIK2 expression should be tightly controlled in retina so hyperglycemia cannot cause alteration in SIK2 protein level. From a different viewpoint, it may be the case that upregulation in SIK2 expression can occur in a later time. In addition, immunohistochemical stainings of the retinal sections performed with anti-SIK2 antibody demonstrated that SIK2 strongly expressed in the cell bodies in INL and GCL but no labeling was detected in photoreceptor layer. Comparison of diabetic and control retinae suggests that there was no change in the expression pattern of SIK2 in the retina as well within this time frame of diabetes.

The modulations of SIK2 kinase activity in retina within the first 8-weeks of diabetes were traced through changes in autophosphorylation levels by using non-radioactive phosphatase-coupled Universal Kinase Activity Kit. The result indicates that SIK2 showed an increased activity in 2-week and 4-week diabetic retina compared to controls but no increase was detectable in 8-week diabetic retina. The increase in SIK2 activity is not statistically significant but meaningful showing consistency with the earlier report that demonstrated the increase in SIK2 activity in 2-week diabetic retina (Küser-Abalı *et al*., 2013). Therefore, the kinase assay needs to be repeated to reach a significant conclusion

for the better characterization of SIK2 activity in this time frame of diabetes.

It should be taken into consideration that SIK2 is not the only enzyme that serine phosphorylates IRS1. There are evidences suggesting that some downstream effectors of PI3K such as IKKβ and mTOR phosphorylate IRS1 on serine residues indicating a control mechanism of PI3K to negatively regulate IRS1 function in insulin signaling (Liu *et al*., 2004). In addition, it has been reported that TNFα induces the phosphorylation of IRS1 on the serine residue thus inhibits insulin signaling and triggers apoptosis in Müller cells cultured under hyperglycemia (Walker *et al*., 2011). Therefore, it can be claimed that SIK2 may contribute to insulin resistance and cell death in diabetic retina not by itself but together with other IRS1 upstream serine kinases; however, no comprehensive mechanism has been elucidated yet.

In order to further characterize the role of SIK2, the interaction between SIK2 and its substrate IRS1 was analyzed in diabetic retina. Co-IP assays showed that, for the first time to the best of our knowledge, SIK2 and IRS1 directly interacted in the retina and this interaction was enhanced by hyperglycemia beginning from the 4^{th} week of diabetes, parallel with the cell death profile of diabetic retina. When the expression, activity and interaction profile of SIK2 with IRS1 are taken together, it is obvious that SIK2 is not involved in the progression of DR via its altered expression within the first 8 weeks of diabetes. However the increase in the activity of SIK2 by the 2^{nd} week of diabetes and enhanced interaction with IRS1 by the 4^{th} week of diabetes might be significant to enlighten the mechanism leading to cell death. On the other hand, the reason why SIK2 activity shows no change in the 8^{th} week of diabetes, in which cell death was densely observed, needs an explanation. It might be the case that the increase in the activity of SIK2 or other upstream serine kinases of IRS1 could lead to cell death not instantly but some time later suggesting the need of a prolonged effect of activity to trigger cell death. The possibility of selective loss of retinal cells, in which SIK2 showed increased activity, could uncover activity change of SIK2 in the diabetic retina at that time. However, due to the lack of an antibody that recognizes overactive SIK2 *in vivo*, we are unable to trace and verify that. Additionally, SIK2 activity and cell death profile should be monitored also in the time interval between the 4^{th} and 8^{th} week of diabetes. The possibility that SIK2 activity could have been transiently increased until the 8^{th} week should not be ignored.

In conclusion, in the view of current information, we cannot directly correlate SIK2 with DR. Under hyperglycemia, increase in SIK2 activity and interaction with IRS1 in the retina can lead to impairment of insulin-induced survival pathway via negative regulation of IRS1. Overactive SIK2 can phosphorylate more and more IRS1 on the specific residue, serine 789 (Horike *et al*., 2003). However, the antibody for p-IRS1 s789 did not work properly in Western Blot analysis of retinal samples thus further optimization is necessary. Although we were not able to show enhanced IRS1 serine phosphorylation in diabetic retina in this project, it has been previously reported that serine phosphorylation of IRS1 increases while tyrosine phosphorylation decreases, hampering Akt activation in cultured Müller cells under hyperglycemia (Küser-Abalı *et al*., 2013). Inactive Akt cannot support survival and eventually may cause retinal degeneration and blindness. In order to support our proposed hypothesis, SIK2 activity, IRS1 and Akt phosphorylation profiles should be analyzed in detail also in diabetic retina.

In the retina, insulin-induced survival pathway could be under the strict control of tissue's own regulation mechanism affected by many downstream and upstream regulators therefore the mechanism leading to apoptosis in diabetic retina awaits further investigation. In order to observe direct effect of SIK2 in DR, the experiments with the tissue-specific SIK2 knockdown or knockout diabetic models should be performed. It is promising that in the light of new evidences and further experiments revealing the underlying mechanism, SIK2 could serve a new potential target molecule to develop new treatments for DR.

REFERENCES

Barber, A. J., D. A. Antonetti, and T. W. Gardner, 2000, "Altered Expression of Retinal Occludin and Glial Fibrillary Acidic Protein in Experimental Diabetes. The Penn State Retina Research Group", *Investigative Ophthalmology and Visual Science,* Vol. 41, No. 11, pp. 3561-3568.

Barber, A. J., D. A. Antonetti, T. S. Kern, C. E. Reiter, R. S. Soans, J. K. Krady, S. W. Levison, T. W. Gardner, and S. K. Bronson, 2005, "The Ins2akita Mouse as a Model of Early Retinal Complications in Diabetes", *Invest Ophthalmology and Visual Science,* Vol. 46, No. 6, pp. 2210-2218.

Barber, A. J., E. Lieth, S. A. Khin, D. A. Antonetti, A. G. Buchanan, and T. W. Gardner, 1998, "Neural Apoptosis in the Retina During Experimental and Human Diabetes. Early Onset and Effect of Insulin", *Journal of Clinical Investigation,* Vol. 102, No. 4, pp. 783-791.

Bedoya, F. J., F. Solano, and M. Lucas, 1996, "N-Monomethyl-Arginine and Nicotinamide Prevent Streptozotocin-Induced Double Strand DNA Break Formation in Pancreatic Rat Islets", *Experientia,* Vol. 52, No. 4, pp. 344-347.

Berdeaux, R., N. Goebel, L. Banaszynski, H. Takemori, T. Wandless, G. D. Shelton, and M. Montminy, 2007, "Sik1 Is a Class Ii Hdac Kinase That Promotes Survival of Skeletal Myocytes", *Nature Medicine,* Vol. 13, No. 5, pp. 597-603.

Bignami, A., and D. Dahl, 1979, "The Radial Glia of Muller in the Rat Retina and Their Response to Injury. An Immunofluorescence Study with Antibodies to the Glial Fibrillary Acidic (Gfa) Protein", *Experimental Eye Research,* Vol. 28, No. 1, pp. 63-69.

Bolaffi, J. L., S. Nagamatsu, J. Harris, and G. M. Grodsky, 1987, "Protection by Thymidine, an Inhibitor of Polyadenosine Diphosphate Ribosylation, of

Streptozotocin Inhibition of Insulin Secretion", *Endocrinology,* Vol. 120, No. 5, pp. 2117-2122.

Boura-Halfon, S., and Y. Zick, 2009, "Phosphorylation of Irs Proteins, Insulin Action, and Insulin Resistance", *American Journal of Physiology, Endocrinology and Metabolism,* Vol. 296, No. 4, pp. E581-591.

Bricambert, J., J. Miranda, F. Benhamed, J. Girard, C. Postic, and R. Dentin, 2010, "Salt-Inducible Kinase 2 Links Transcriptional Coactivator P300 Phosphorylation to the Prevention of Chrebp-Dependent Hepatic Steatosis in Mice", *Journal of Clinical Investigation,* Vol. 120, No. 12, pp. 4316-4331.

Bringmann, A., T. Pannicke, J. Grosche, M. Francke, P. Wiedemann, S. N. Skatchkov, N. N. Osborne, and A. Reichenbach, 2006, "Muller Cells in the Healthy and Diseased Retina", *Progress in Retina and Eye Research,* Vol. 25, No. 4, pp. 397-424.

Bringmann, A., and A. Reichenbach, 2001, "Role of Muller Cells in Retinal Degenerations", *Frontiers in Bioscience,* Vol. 6, No. 3, pp. E72-92.

Bringmann, A., A. Reichenbach, and P. Wiedemann, 2004, "Pathomechanisms of Cystoid Macular Edema", *Ophthalmic Research,* Vol. 36, No. 5, pp. 241-249.

Centanin, L., and J. Wittbrodt, 2014, "Retinal Neurogenesis", *Development,* Vol. 141, No. 2, pp. 241-244.

Chang, F., J. T. Lee, P. M. Navolanic, L. S. Steelman, J. G. Shelton, W. L. Blalock, R. A. Franklin, and J. A. McCubrey, 2003, "Involvement of Pi3k/Akt Pathway in Cell Cycle Progression, Apoptosis, and Neoplastic Transformation: A Target for Cancer Chemotherapy", *Leukemia,* Vol. 17, No. 3, pp. 590-603.

Chen, W. S., P. Z. Xu, K. Gottlob, M. L. Chen, K. Sokol, T. Shiyanova, I. Roninson, W. Weng, R. Suzuki, K. Tobe, T. Kadowaki, N. Hay, 2001, "Growth Retardation and Increased Apoptosis in Mice with Homozygous Disruption of the Akt1 Gene",

Genes and Development, Vol. 15, No. 17, pp. 2203-2208.

Cleland, W. W., 1964, "Dithiothreitol, a New Protective Reagent for Sh Groups", *Biochemistry,* Vol. 3, No.4, pp. 480-482.

Considine, R. V., M. R. Nyce, L. E. Allen, L. M. Morales, S. Triester, J. Serrano, J. Colberg, S. Lanza-Jacoby, and J. F. Caro, 1995, "Protein Kinase C Is Increased in the Liver of Humans and Rats with Non-Insulin-Dependent Diabetes Mellitus: An Alteration Not Due to Hyperglycemia", *Journal of Clinical Investigation,* Vol. 95, No. 6, pp. 2938-2944.

Czech, M. P., 1985, "The Nature and Regulation of the Insulin Receptor: Structure and Function", *Annual Review of Physiology,* Vol. 47, No. 3, pp. 357-381.

Das, A., B. Pansky, and G. C. Budd, 1987, "Demonstration of Insulin-Specific Mrna in Cultured Rat Retinal Glial Cells", *Investigative Ophthalmology and Visual Science,* Vol. 28, No. 11, pp. 1800-1810.

Deeds, M. C., J. M. Anderson, A. S. Armstrong, D. A. Gastineau, H. J. Hiddinga, A. Jahangir, N. L. Eberhardt, and Y. C. Kudva, 2011, "Single Dose Streptozotocin-Induced Diabetes: Considerations for Study Design in Islet Transplantation Models", *Laboratory Animals,* Vol. 45, No. 3, pp. 131-140.

Dentin, R., Y. Liu, S. H. Koo, S. Hedrick, T. Vargas, J. Heredia, J. Yates, 3rd, and M. Montminy, 2007, "Insulin Modulates Gluconeogenesis by Inhibition of the Coactivator Torc2", *Nature,* Vol. 449, No. 7160, pp. 366-369.

Du, Y., C. M. Miller, and T. S. Kern, 2003, "Hyperglycemia Increases Mitochondrial Superoxide in Retina and Retinal Cells", *Free Radical Biology and Medicine,* Vol. 35, No. 11, pp. 1491-1499.

Dummler, B., and B. A. Hemmings, 2007, "Physiological Roles of Pkb/Akt Isoforms in Development and Disease", *Biochemical Society Transactions,* Vol. 35, No. Pt 2,

pp. 231-235.

Eisenfeld, A. J., A. H. Bunt-Milam, and P. V. Sarthy, 1984, "Muller Cell Expression of Glial Fibrillary Acidic Protein after Genetic and Experimental Photoreceptor Degeneration in the Rat Retina", *Investigative Ophthalmology and Visual Science,* Vol. 25, No. 11, pp. 1321-1328.

El-Bab, M. F., N. S. Zaki, M. A. Mojaddidi, M. Al-Barry, and H. A. El-Beshbishy, 2013, "Diabetic Retinopathy Is Associated with Oxidative Stress and Mitigation of Gene Expression of Antioxidant Enzymes", *International Journal of General Medicine,* Vol. 6, No. 3, pp. 799-806.

Engelgau, M. M., L. S. Geiss, J. B. Saaddine, J. P. Boyle, S. M. Benjamin, E. W. Gregg, E. F. Tierney, N. Rios-Burrows, A. H. Mokdad, E. S. Ford, G. Imperatore, V. Narayan, 2004, "The Evolving Diabetes Burden in the United States", *Annals of Internal Medicine,* Vol. 140, No. 11, pp. 945-950.

Garcia, M., and E. Vecino, 2003, "Role of Muller Glia in Neuroprotection and Regeneration in the Retina", *Histology and Histopathology,* Vol. 18, No. 4, pp. 1205-1218.

Gosbell, A. D., I. Favilla, K. M. Baxter, and P. Jablonski, 2000, "Insulin Receptor and Insulin Receptor Substrate-I in Rat Retinae", *Clinical and Experimental Ophthalmology,* Vol. 28, No. 3, pp. 212-215.

Gual, P., Y. Le Marchand-Brustel, and J. F. Tanti, 2005, "Positive and Negative Regulation of Insulin Signaling through Irs-1 Phosphorylation", *Biochimie,* Vol. 87, No. 1, pp. 99-109.

Hammes, H. P., H. J. Federoff, and M. Brownlee, 1995, "Nerve Growth Factor Prevents Both Neuroretinal Programmed Cell Death and Capillary Pathology in Experimental Diabetes", *Molecular Medicine,* Vol. 1, No. 5, pp. 527-534.

Hashimoto, Y. K., T. Satoh, M. Okamoto, and H. Takemori, 2008, "Importance of Autophosphorylation at Ser186 in the a-Loop of Salt Inducible Kinase 1 for Its Sustained Kinase Activity", *Journal of Cellular Biochemistry,* Vol. 104, No. 5, pp. 1724-1739.

Hernandez-Sanchez, C., A. Lopez-Carranza, C. Alarcon, E. J. de La Rosa, and F. de Pablo, 1995, "Autocrine/Paracrine Role of Insulin-Related Growth Factors in Neurogenesis: Local Expression and Effects on Cell Proliferation and Differentiation in Retina", *Proceedings of the National Academy of Sciences of the United States of America,* Vol. 92, No. 21, pp. 9834-9838.

Hoon, M., H. Okawa, L. Della Santina, and R. O. Wong, 2014, "Functional Architecture of the Retina: Development and Disease", *Progress in Retina and Eye Research,* Vol. 42, No. 1, pp. 44-84.

Horike, N., H. Takemori, Y. Katoh, J. Doi, L. Min, T. Asano, X. J. Sun, H. Yamamoto, S. Kasayama, M. Muraoka, Y. Nonaka, M. Okamoto, 2003, "Adipose-Specific Expression, Phosphorylation of Ser794 in Insulin Receptor Substrate-1, and Activation in Diabetic Animals of Salt-Inducible Kinase-2", *Journal of Biological Chemistry,* Vol. 278, No. 20, pp. 18440-18447.

Jayaguru, P., and S. Mohr, 2011, "Nuclear Gapdh: Changing the Fate of Muller Cells in Diabetes", *Journal of Ocular Biology, Diseases and Informatics,* Vol. 4, No. 1-2, pp. 34-41.

Jiang, Y., J. Pagadala, D. Miller, and J. J. Steinle, 2013, "Reduced Insulin Receptor Signaling in Retinal Muller Cells Cultured in High Glucose", *Molecular Vision,* Vol. 19, No. 2, pp. 804-811.

Kanzaki, M., and J. E. Pessin, 2001, "Signal Integration and the Specificity of Insulin Action", *Cellular Biochemistry and Biophysics,* Vol. 35, No. 2, pp. 191-209.

Katoh, Y., H. Takemori, N. Horike, J. Doi, M. Muraoka, L. Min, and M. Okamoto, 2004,

"Salt-Inducible Kinase (Sik) Isoforms: Their Involvement in Steroidogenesis and Adipogenesis", *Molecular and Cellular Endocrinology,* Vol. 217, No. 1-2, pp. 109-112.

Katz, M. L., and G. E. Eldred, 1989, "Retinal Light Damage Reduces Autofluorescent Pigment Deposition in the Retinal Pigment Epithelium", *Investigative Ophthalmology and Visual Science,* Vol. 30, No. 1, pp. 37-43.

Kerouz, N. J., D. Horsch, S. Pons, and C. R. Kahn, 1997, "Differential Regulation of Insulin Receptor Substrates-1 and -2 (Irs-1 and Irs-2) and Phosphatidylinositol 3-Kinase Isoforms in Liver and Muscle of the Obese Diabetic (Ob/Ob) Mouse", *Journal of Clinical Investigation,* Vol. 100, No. 12, pp. 3164-3172.

Kertes, P. J., and T. M. Johnson, 2007, *Evidence-Based Eye Care*, Lippincott Williams & Wilkins, Philadelphia, PA, USA.

Kolb, H., 2003, "How the Retina Works", *American Scientist*, Vol. 91, No. 3, pp. 28-35.

Koo, S. H., L. Flechner, L. Qi, X. Zhang, R. A. Screaton, S. Jeffries, S. Hedrick, W. Xu, F. Boussouar, P. Brindle, H. Takemori, M. Montminy, 2005, "The Creb Coactivator Torc2 Is a Key Regulator of Fasting Glucose Metabolism", *Nature,* Vol. 437, No. 7062, pp. 1109-1111.

Kowluru, R. A., R. L. Engerman, G. L. Case, and T. S. Kern, 2001, "Retinal Glutamate in Diabetes and Effect of Antioxidants", *Neurochemistry International,* Vol. 38, No. 5, pp. 385-390.

Küser, G., 2011, *SIK2: A Key Player in FGF2-Induced Proliferation and Insulin Induced Survival/Hyperglycemia-Dependent Apoptosis in Müller Cells*, Ph.D. Thesis, Boğaziçi University.

Küser-Abalı, G., F. Ozcan, A. Ugurlu, A. Uysal, S. H. Fuss, and K. Bugra-Bilge, 2013, "SIK2 Is Involved in the Negative Modulation of Insulin-Dependent Müller Cell

Survival and Implicated in Hyperglycemia-Induced Cell Death", Investigative Ophthalmology and Visual Science, Vol. 54, No. 5, pp. 3526-3537.

Lieth, E., A. J. Barber, B. Xu, C. Dice, M. J. Ratz, D. Tanase, and J. M. Strother, 1998, "Glial Reactivity and Impaired Glutamate Metabolism in Short-Term Experimental Diabetic Retinopathy. Penn State Retina Research Group", *Diabetes,* Vol. 47, No. 5, pp. 815-820.

Lieth, E., K. F. LaNoue, D. A. Antonetti, and M. Ratz, 2000, "Diabetes Reduces Glutamate Oxidation and Glutamine Synthesis in the Retina. The Penn State Retina Research Group", *Experimental Eye Research,* Vol. 70, No. 6, pp. 723-730.

Liu, Y. F., A. Herschkovitz, S. Boura-Halfon, D. Ronen, K. Paz, D. Leroith, and Y. Zick, 2004, "Serine Phosphorylation Proximal to Its Phosphotyrosine Binding Domain Inhibits Insulin Receptor Substrate 1 Function and Promotes Insulin Resistance", *Molecular and Cellular Biology,* Vol. 24, No. 21, pp. 9668-9681.

Liu, Y. F., K. Paz, A. Herschkovitz, A. Alt, T. Tennenbaum, S. R. Sampson, M. Ohba, T. Kuroki, D. LeRoith, and Y. Zick, 2001, "Insulin Stimulates Pkczeta -Mediated Phosphorylation of Insulin Receptor Substrate-1 (Irs-1). A Self-Attenuated Mechanism to Negatively Regulate the Function of Irs Proteins", *Journal of Biological Chemistry,* Vol. 276, No. 17, pp. 14459-14465.

Lizcano, J. M., O. Goransson, R. Toth, M. Deak, N. A. Morrice, J. Boudeau, S. A. Hawley, L. Udd, T. P. Makela, D. G. Hardie, D. R. Alessi, 2004, "Lkb1 Is a Master Kinase That Activates 13 Kinases of the Ampk Subfamily, Including Mark/Par-1", *EMBO Journal,* Vol. 23, No. 4, pp. 833-843.

Madonna, R., and R. De Caterina, 2012, "Atherogenesis and Diabetes: Focus on Insulin Resistance and Hyperinsulinemia", *Revista Espanola de Cardiologia (Engl Ed),* Vol. 65, No. 4, pp. 309-313.

Martin, P. M., P. Roon, T. K. Van Ells, V. Ganapathy, and S. B. Smith, 2004, "Death of

Retinal Neurons in Streptozotocin-Induced Diabetic Mice", *Investigative Ophthalmology and Visual Science,* Vol. 45, No. 9, pp. 3330-3336.

Medina, E. A., R. R. Afsari, T. Ravid, S. S. Castillo, K. L. Erickson, and T. Goldkorn, 2005, "Tumor Necrosis Factor-{Alpha} Decreases Akt Protein Levels in 3t3-L1 Adipocytes Via the Caspase-Dependent Ubiquitination of Akt", *Endocrinology,* Vol. 146, No. 6, pp. 2726-2735.

Miyamoto, K., S. Khosrof, S. E. Bursell, R. Rohan, T. Murata, A. C. Clermont, L. P. Aiello, Y. Ogura, and A. P. Adamis, 1999, "Prevention of Leukostasis and Vascular Leakage in Streptozotocin-Induced Diabetic Retinopathy Via Intercellular Adhesion Molecule-1 Inhibition", *Proceedings of National Academy of Sciences United States of America,* Vol. 96, No. 19, pp. 10836-10841.

Mizutani, M., C. Gerhardinger, and M. Lorenzi, 1998, "Muller Cell Changes in Human Diabetic Retinopathy", *Diabetes,* Vol. 47, No. 3, pp. 445-449.

Mizutani, M., T. S. Kern, and M. Lorenzi, 1996, "Accelerated Death of Retinal Microvascular Cells in Human and Experimental Diabetic Retinopathy", *Journal of Clinical Investigation,* Vol. 97, No. 12, pp. 2883-2890.

Mothe, I., and E. Van Obberghen, 1996, "Phosphorylation of Insulin Receptor Substrate-1 on Multiple Serine Residues, 612, 632, 662, and 731, Modulates Insulin Action", *Journal of Biological Chemistry,* Vol. 271, No. 19, pp. 11222-11227.

Newman, E. A., 1996, "Acid Efflux from Retinal Glial Cells Generated by Sodium Bicarbonate Cotransport", *Journal of Neuroscience,* Vol. 16, No. 1, pp. 159-168.

Nukatsuka, M., Y. Yoshimura, M. Nishida, and J. Kawada, 1990, "Importance of the Concentration of Atp in Rat Pancreatic Beta Cells in the Mechanism of Streptozotocin-Induced Cytotoxicity", *Journal of Endocrinology,* Vol. 127, No. 1, pp. 161-165.

Okamoto, M., H. Takemori, and Y. Katoh, 2004, "Salt-Inducible Kinase in Steroidogenesis and Adipogenesis", *Trends in Endocrinology and Metabolism,* Vol. 15, No. 1, pp. 21-26.

Ola, M. S., K. Hosoya, and K. F. LaNoue, 2011, "Influence of Insulin on Glutamine Synthetase in the Muller Glial Cells of Retina", *Metabolic Brain Disease,* Vol. 26, No. 3, pp. 195-202.

Ola, M. S., M. I. Nawaz, M. M. Siddiquei, S. Al-Amro, and A. M. Abu El-Asrar, 2012, "Recent Advances in Understanding the Biochemical and Molecular Mechanism of Diabetic Retinopathy", *Journal of Diabetes Complications,* Vol. 26, No. 1, pp. 56-64.

Oshitari, T., and S. Roy, 2005, "Diabetes: A Potential Enhancer of Retinal Injury in Rat Retinas", *Neuroscience Letters,* Vol. 390, No. 1, pp. 25-30.

Park, S. H., J. W. Park, S. J. Park, K. Y. Kim, J. W. Chung, M. H. Chun, and S. J. Oh, 2003, "Apoptotic Death of Photoreceptors in the Streptozotocin-Induced Diabetic Rat Retina", *Diabetologia,* Vol. 46, No. 9, pp. 1260-1268.

Pederson, T. M., D. L. Kramer, and C. M. Rondinone, 2001, "Serine/Threonine Phosphorylation of Irs-1 Triggers Its Degradation: Possible Regulation by Tyrosine Phosphorylation", *Diabetes,* Vol. 50, No. 1, pp. 24-31.

Pessin, J. E., and A. R. Saltiel, 2000, "Signaling Pathways in Insulin Action: Molecular Targets of Insulin Resistance", *Journal of Clinical Investigation,* Vol. 106, No. 2, pp. 165-169.

Pow, D. V., and S. R. Robinson, 1994, "Glutamate in Some Retinal Neurons Is Derived Solely from Glia", *Neuroscience,* Vol. 60, No. 2, pp. 355-366.

Qiao, L. Y., R. Zhande, T. L. Jetton, G. Zhou, and X. J. Sun, 2002, "In Vivo Phosphorylation of Insulin Receptor Substrate 1 at Serine 789 by a Novel Serine

Kinase in Insulin-Resistant Rodents", *Journal of Biological Chemistry,* Vol. 277, No. 29, pp. 26530-26539.

Rajala, R. V., B. Wiskur, M. Tanito, M. Callegan, and A. Rajala, 2009, "Diabetes Reduces Autophosphorylation of Retinal Insulin Receptor and Increases Protein-Tyrosine Phosphatase-1b Activity", *Investigative Ophthalmology and Visual Science,* Vol. 50, No. 3, pp. 1033-1040.

Reiter, C. E., and T. W. Gardner, 2003, "Functions of Insulin and Insulin Receptor Signaling in Retina: Possible Implications for Diabetic Retinopathy", *Progress in Retina and Eye Research,* Vol. 22, No. 4, pp. 545-562.

Ricort, J. M., J. F. Tanti, E. Van Obberghen, and Y. Le Marchand-Brustel, 1995, "Alterations in Insulin Signalling Pathway Induced by Prolonged Insulin Treatment of 3t3-L1 Adipocytes", *Diabetologia,* Vol. 38, No. 10, pp. 1148-1156.

Rieke, F., and D. A. Baylor, 1998, "Origin of Reproducibility in the Responses of Retinal Rods to Single Photons", *Biophysics Journal,* Vol. 75, No. 4, pp. 1836-1857.

Rungger-Brandle, E., A. A. Dosso, and P. M. Leuenberger, 2000, "Glial Reactivity, an Early Feature of Diabetic Retinopathy", *Investigative Ophthalmology and Visual Science,* Vol. 41, No. 7, pp. 1971-1980.

Saltiel, A. R., and C. R. Kahn, 2001, "Insulin Signalling and the Regulation of Glucose and Lipid Metabolism", *Nature,* Vol. 414, No. 6865, pp. 799-806.

Sarthy, V., and H. Ripps, 2001, *The Retinal Müller Cell*, Kluwer Academics/Plenum Publishers, New York, NY, USA.

Schiller, P. H., 2010, "Parallel Information Processing Channels Created in the Retina", *Proceedings of National Academy of Sciences United States of America,* Vol. 107, No. 40, pp. 17087-17094.

Schnedl, W. J., S. Ferber, J. H. Johnson, and C. B. Newgard, 1994, "Stz Transport and Cytotoxicity. Specific Enhancement in Glut2-Expressing Cells", *Diabetes,* Vol. 43, No. 11, pp. 1326-1333.

Screaton, R. A., M. D. Conkright, Y. Katoh, J. L. Best, G. Canettieri, S. Jeffries, E. Guzman, S. Niessen, J. R. Yates, 3rd, H. Takemori, M. Okamoto, M. Montminy, 2004, "The Creb Coactivator Torc2 Functions as a Calcium- and Camp-Sensitive Coincidence Detector", *Cell,* Vol. 119, No. 1, pp. 61-74.

Shen, X., Y. Zhong, B. Xie, Y. Cheng, and Q. Jiao, 2010, "Pigment Epithelium Derived Factor as an Anti-Inflammatory Factor against Decrease of Glutamine Synthetase Expression in Retinal Muller Cells under High Glucose Conditions", *Graefes Archive for Clinical and Experimental Ophthalmology,* Vol. 248, No. 8, pp. 1127-1136.

Smith, R. S., S. W. M. John, P. M. Nishina, and J. P. Sundberg, 2002, *Systematic Evaluation of the Mouse Eye: Anatomy, Pathology and Biomethods*, CRC Press LLC, Boca Raton, Florida, FL, USA.

Stephens, J. M., J. Lee, and P. F. Pilch, 1997, "Tumor Necrosis Factor-Alpha-Induced Insulin Resistance in 3t3-L1 Adipocytes Is Accompanied by a Loss of Insulin Receptor Substrate-1 and Glut4 Expression without a Loss of Insulin Receptor-Mediated Signal Transduction", *Journal of Biological Chemistry,* Vol. 272, No. 2, pp. 971-976.

Sun, X. J., D. L. Crimmins, M. G. Myers, Jr., M. Miralpeix, and M. F. White, 1993, "Pleiotropic Insulin Signals Are Engaged by Multisite Phosphorylation of Irs-1", *Molecular and Cellular Biology,* Vol. 13, No. 12, pp. 7418-7428.

Szkudelski, T., 2001, "The Mechanism of Alloxan and Streptozotocin Action in B Cells of the Rat Pancreas", *Physiological Research,* Vol. 50, No. 6, pp. 537-546.

Taniguchi, C. M., B. Emanuelli, and C. R. Kahn, 2006, "Critical Nodes in Signalling

Pathways: Insights into Insulin Action", *Nature Reviews Molecular Cell Biology,* Vol. 7, No. 2, pp. 85-96.

Vivanco, I., and C. L. Sawyers, 2002, "The Phosphatidylinositol 3-Kinase Akt Pathway in Human Cancer", *Nature Reviews Cancer,* Vol. 2, No. 7, pp. 489-501.

Walker, R. J., N. M. Anderson, Y. Jiang, S. Bahouth, and J. J. Steinle, 2011, "Role of Beta-Adrenergic Receptor Regulation of Tnf-Alpha and Insulin Signaling in Retinal Muller Cells", *Investigative Ophthalmology and Visual Science,* Vol. 52, No. 13, pp. 9527-9533.

Wei, M., L. Ong, M. T. Smith, F. B. Ross, K. Schmid, A. J. Hoey, D. Burstow, and L. Brown, 2003, "The Streptozotocin-Diabetic Rat as a Model of the Chronic Complications of Human Diabetes", *Heart, Lung and Circulation,* Vol. 12, No. 1, pp. 44-50.

Weinstein, D. E., M. L. Shelanski, and R. K. Liem, 1991, "Suppression by Antisense Mrna Demonstrates a Requirement for the Glial Fibrillary Acidic Protein in the Formation of Stable Astrocytic Processes in Response to Neurons", *Journal of Cell Biology,* Vol. 112, No. 6, pp. 1205-1213.

Williams, R., M. Airey, H. Baxter, J. Forrester, T. Kennedy-Martin, and A. Girach, 2004, "Epidemiology of Diabetic Retinopathy and Macular Oedema: A Systematic Review", *Eye (London),* Vol. 18, No. 10, pp. 963-983.

Xi, X., L. Gao, D. A. Hatala, D. G. Smith, M. C. Codispoti, B. Gong, T. S. Kern, and J. Z. Zhang, 2005, "Chronically Elevated Glucose-Induced Apoptosis Is Mediated by Inactivation of Akt in Cultured Muller Cells", *Biochemical and Biophysical Research Communications,* Vol. 326, No. 3, pp. 548-553.

Xu, J., L. Zhang, A. Chou, T. Allaby, G. Belanger, J. Radziuk, B. J. Jasmin, T. Miki, S. Seino, and J. M. Renaud, 2008, "Katp Channel-Deficient Pancreatic Beta-Cells Are Streptozotocin Resistant Because of Lower Glut2 Activity", *American Journal of*

Physiology, Endocrinology and Metabolism, Vol. 294, No. 2, pp. E326-335.

Yang, F. C., Y. H. Lin, W. H. Chen, J. Y. Huang, H. Y. Chang, S. H. Su, H. T. Wang, C. Y. Chiang, P. H. Hsu, M. D. Tsai, B. Chin, M. Tan, S. C. Lee, 2013, "Interaction between Salt-Inducible Kinase 2 (Sik2) and P97/Valosin-Containing Protein (Vcp) Regulates Endoplasmic Reticulum (Er)-Associated Protein Degradation in Mammalian Cells", *Journal of Biological Chemistry,* Vol. 288, No. 47, pp. 33861-33872.

Yau, J. W., S. L. Rogers, R. Kawasaki, E. L. Lamoureux, J. W. Kowalski, T. Bek, S. J. Chen, J. M. Dekker, A. Fletcher, J. Grauslund, S. Haffner, R. F. Hamman, M. K. Ikram, T. Kayama, B. E. K. Klein, R. Klein, S. Krishnaiah, K. Mayurasakorn, J. P. O'hare, T. J. Orchard, M. Porta, M. Rema, M. S. Roy, T. Sharma, J. Shaw, H. Taylor, J. M. Tielsch, R. Varma, J. J. Wang, N. Wang, S. West, L. Xu, M. Yasuda, X. Zhang, P. Mitchell, T. Y. Wong, 2012, "Global Prevalence and Major Risk Factors of Diabetic Retinopathy", *Diabetes Care,* Vol. 35, No. 3, pp. 556-564.

Zeng, X. X., Y. K. Ng, and E. A. Ling, 2000, "Neuronal and Microglial Response in the Retina of Streptozotocin-Induced Diabetic Rats", *Visual Neuroscience,* Vol. 17, No. 3, pp. 463-471.

Zick, Y., 2005, "Ser/Thr Phosphorylation of Irs Proteins: A Molecular Basis for Insulin Resistance", *Science STKE [Signal Transduction Knowledge Environment],* Vol. 2005, No. 268, pp. pe4